University of South Bohemia in České Budějovice

Faculty of Science

# The role of Ervl in the mitochondrial import machinery and iron sulphur cluster export machinery in *Trypanosoma brucei*

Bachelor thesis

Michala Boudová

Supervisor: Mgr. Haindrich Alexander Christoph, MSc.

České Budějovice, 2016

Boudová, M., 2016: The role of Ervl in the mitochondrial import machinery and iron sulphur cluster export machinery in *Trypanosoma brucei*. Bc. Thesis, in English. - 54 p, Faculty of Science, University of South Bohemia, České Budějovice, Czech Republic.

**Annotation**

The aim of this thesis was to determine the subcellular localization of Erv1 and to verify its involvement in the cytosolic iron sulphur cluster assembly. Additionally a search for potential interaction partners was conducted, which could possibly assist Erv1 in the processes where it was suggested to take a part, so either in the biogenesis of iron-sulphur cluster proteins or in the mitochondrial protein import, in procyclic *T. brucei*.

**Affirmation**

I hereby declare that, in accordance with Article 47b of Act No. 111/1998 in the valid wording, I agree with the publication of my bachelor thesis, in full to be kept in the Faculty of Science archive, in electronic form in publicly accessible part of STAG database operated by the University of South Bohemia in České Budějovice accessible through its web pages. Further, I agree to the electronic publication of the comments of my supervisor and thesis opponents and the record of the proceedings and results of the thesis defence in accordance with aforementioned Act. No. 111/1998. I also agree to the comparison of the text of my thesis with the Thesis.cz thesis database operated by the National Registry of University and a plagiarism detection system.

České Budějovice, 21. 4. 2016

……..

Michala Boudová

**Acknowledgements**

First of all, I would like to thank prof. Julius Lukeš for the great opportunity to work in his laboratory and also for his support in completing this project.

I am highly indebted to my supervisor Alex for the kind guidance and his infinite patience which has led me through the whole process and helped me to overcome many tough situations such as finishing this work itself. I would like to express my gratitude for all the time and effort he has dedicated to me, for all the valuable discussions that helped me better understand my area of research, for enforcing strict validations of the results, and thus teaching me how to do a research. I have been amazingly fortunate to have such an advisor, who gave me the freedom to explore on my own, so that I could learn from my mistakes. At the same time he was always there when my steps faltered. I am also thankful to him for carefully reading and commenting on countless revisions of this thesis.

My thanks and appreciations also go to Eva H., my group leader who provided vital insights and expertise that greatly assisted the research, I am very thankful to her for the discussions, practical advices and the encouragement she gave me.

I would like to acknowledge everyone, who directly or indirectly, have lend a helping hand, especially Priscila for her constructively critical reminders, Drahuška and Zdeněk whose office was always opened whenever I ran into a trouble spot, or Josef who was so kind and constantly shared his laboratory equipment with me. I would like to extend my sincere thanks to all the members of Lukeš lab, as all of them were always willing to help me anytime I was in need.

Finally I must express my very profound gratitude to my family for providing me with unfailing support and continuous encouragement throughout my years of study and through the process of researching and writing this thesis. This accomplishment would have not been possible without them.

**Abbreviations**

| | |
|---|---|
| [Fe-S] | Iron-sulphur cluster |
| ABC trnasporter | ATP binding cassette transporter |
| *A. thaliana* (At) | *Arabidopsis thaliana* |
| ATP | Adenosine triphosphate |
| bp | Base pair |
| CIA | Cytosolic assembly machinery |
| CPC | Cysteine-Proline-Cysteine |
| cyt c | Cytochrome c |
| DAPI | 4',6-diamidino-2-phenylindole |
| DNA | Deoxyribonucleic acid |
| EtBr | Ethidium bromide |
| FAD | Flavine adenine dinucleotide |
| Hsp | Heat shock protein |
| IFA | Immunofluorescence assay |
| IMS | Intermembrane space of mitochondria |
| ISC | Iron sulphur cluster assembly machinery |
| ITS | IMS-targeting signal |
| kDa | Kilodalton |
| KISS | Kinetoplastida-specific second (domain) |
| *L. tarentolae* (Lt) | *Leshmania tarentolae* |
| Leu-Pro-Pro-Val-Lys | Leucine-Proline-Proline-Valine-Lysine |
| MIA | Mitochondrial intermembrane space assembly |
| MPI | Mitochondrial protein import |
| NAD(P)H | Nicotinamid adenine dinucleotide phosphate |
| NIF | Nitrogen fixation machinery |
| NTPase | Nucleoside-triphosphatase |
| PAM | Presequence translocase associated motor |
| PBS | Phosphate-buffered saline |
| PCR | Polymerase chain reaction |
| pPOT | PCR only tagging |
| PVDF | Polyvinylidene difluoride |
| RISC | RNA-induced silencing complex |
| RNA | Ribonucleic acid |
| RNAi | RNA interference |
| RT | Room temperature (25°C) |
| *S. cerevisiae* (Sc) | *Saccharomyces cerevisiae* |
| SAM | Sorting and assembly machinery |
| SDM-79 | Semi-defined medium |
| SDS-PAGE | Sodium dodecyl sulfate polyacrylamide gel electrophoresis |
| shRNA | Short hairpin RNA |
| siRNA | Short interfering RNA |
| ss/dsRNA | Single stranded/double stranded RNA |
| SUF | Sulphur-utilization factors system |
| *T. brucei* (Tb) | *Trypanosoma brucei* |
| TIM | Translocase of the inner membrane |
| TOM | Translocase of the outer membrane |
| tRNA | Transfer RNA |
| UV | Ultra violet (light) |

**Table of Contents**

# 1. INTRODUCTION

## 1. 1. *Trypanosoma brucei*

*Trypanosoma brucei* (*T. brucei*), a species of unicellular parasitic protozoa, belongs to the genus *Trypanosoma*, a member of the class Kinetoplastida, phylum Euglenozoa, kingdom Excavata. *T. brucei*, together with related kinetoplastid flagellates causes numerous diseases of man, animals and plants, and thus it is the best studied representative of Excavata, one of the six recognized eukaryotic domains [1].

A large number of species and subspecies of trypanosomes have been described, especially in the equatorial region of the African continent [2]. Different species infect different vertebrates, causing them to suffer from so called trypanosamiasis, also known as sleeping sickness in humans and nagana in animals. Thus these species are economically significant, as they are affecting cattle rearing and agricultural development as well as human health [3]. Shedding the light on the metabolic differences of the parasite to its host, number of novel potential drug targets may be identified [4].

Moreover *T. brucei* is modest to grow under optimized laboratory conditions and has a short generation time. The genome has been completely sequenced [5], and the parasite is amenable to all major methods of both forward and reverse genetics [3]. Trypanosomes actually belong to one of the first organisms in which RNA interference mediated regulation of gene expression was demonstrated [6]. RNAi allows the analysis of genes essential for cell survival, cell cycle regulation, and development, and it is in general easier and faster than gene knockout by homologous recombination [7]. Altogether such characteristics make *T. brucei* a suitable model organism, prominent not only for the investigation of specific pathogenic properties, but also other phenomena, which has lead to additional break-through discoveries of molecular processes such as RNA editing [8] or trans-splicing [9].

*T. brucei* completes its life cycle between an insect (genus *Glossina*) and mammalian hosts (including humans, cattle, horses and wild animals). Different stages of the life cycle show distinct morphology, cellular organisation and thus of course different gene expression and metabolism [10]. The bloodstream stage found in mammalian hosts, are taken up by the insect host during blood meal. Here the parasite enters the midgut, where it rapidly divides, producing the procyclic descendants, which than migrate to the salivary glands. During the next blood meal they become injected, along with the saliva, into the mammalian skin tissue, where they subsequently differentiate into the infective bloodstream form, which can enter the lymphatic system and naturally also the bloodstream. These multiply by binary fission

producing long slender forms that are able to penetrate the blood vessel endothelium and invade extravascular tissues, including the central nervous system [11].

### 1. 2. Iron-Sulphur Cluster proteins

Iron-Sulphur Clusters ([Fe-S]) are chemically versatile inorganic cofactors of numerous proteins, which are involved in a wide variety of cellular processes such as electron transport, enzyme catalysis or regulation of gene expression [12]. Despite the relative simplicity of an [Fe-S] in terms of structure, the assembly and incorporation into apoproteins is assisted by complex cellular machineries. In eukaryotes, such as yeast or human, about 20 components are known so far to facilitate the maturation of [Fe-S] proteins within the cell, and about half of them are encoded by essential genes [13]. These biogenesis components also perform crucial roles in other cellular pathways, e.g. regulation of iron homeostasis or tRNA modification [14]. Numerous neurological and hematological diseases have been associated with defects in [Fe-S] protein biogenesis in humans, e.g. Friedreich's ataxia, myopathy or X-linked sideroblastic anemia with cerebellar ataxia [15].

Most [Fe-S] proteins contain rhombic [2Fe-2S] or cubic [4Fe-4S] clusters, however other forms are known, e.g. [3Fe-4S]. Over the years of research more complex structures were discovered; some clusters include other metals, e.g. molybdenum; and some proteins may contain multiple clusters. The clusters are usually conjugated to the proteins by cysteine ligands [16]. The position of iron inside the cluster where it is conjugated by multiple sulphur atoms allows for an easy change of its oxidation state, making the [Fe-S] proteins ideally suitable for electron transport [17]. Certain [Fe-S]s have the capacity to form spontaneously (under anaerobic conditions), nevertheless such formation of clusters using free $Fe^{2+/3+}$ and $S^{2-}$ could not occur within the cell, due to insufficient concentration and the toxicity of these elements in their free forms and [16]. It is well established that biogenesis *in vivo* is a catalyzed process which requires a participation of multiple proteins [18].

Prokaryotes possess three distinct biosynthetic pathways to generate [Fe-S] proteins; these are the nitrogen-fixation machinery (NIF), the iron sulphur cluster assembly machinery (ISC) and sulphur-utilization factors (SUF) system [19]. Many bacteria harbour ISC and SUF machineries in parallel, others just one of these, and in an anaerobic environment NIF can replace the function of both ISC and SUF, thus the systems are in principle interchangeable [20].

During the course of evolution the ISC assembly machinery in eukaryotes has been inherited from the prokaryotic endosymbiont which gave raise to mitochondria, found within chemotrophic eukaryotes, likewise the SUF system which has been passed to plastids

present in phototrophic eukaryotes [21, 19]. Additionally two eukaryotic-specific machineries have been identified, the ISC export apparatus and the cytosolic [Fe-S] assembly [22]. Thus, not surprisingly, the eukaryotic mitochondrial [Fe-S] proteins show high sequence similarity to bacterial homologues, and naturally they are conserved among all eukaryotes, homologues of the yeast [Fe-S] proteins have been identified in vertebrates, invertebrates, plants and fungi [23].

Therefore in eukaryotes, mitochondria performs a prime role in [Fe-S] protein biogenesis, hence the mitochondrial ISC assembly is involved in maturation of all cellular [Fe-S] proteins [23-26]. More accurately, an unknown sulphur-containing compound coming from the mitochondrial machinery, is (generally believed to be) fundamental for the maturation of nuclear and cytosolic [Fe-S] proteins [18]. Hence the ISC-export machinery together with the cytosolic [Fe-S] assembly machinery (CIA) facilitate the generation of extramitochondrial [Fe-S] proteins exclusively, while the mitochondrial ISC machinery is required for the maturation of [Fe-S] proteins in mitochondria as well as in cytosol [12]. The key principle of the biogenesis of [Fe-S] proteins lies in the assembly of a cluster on a scaffold protein followed by transfer of the cluster to the recipient apoprotein (see Fig.1) [27].

Homologues of the components of the ISC assembly machinery were identified also in species lacking classical mitochondria [28]. These species contain hydrogenosomes or mitosomes, which are double-membrane-bounded organelles that have evolved from mitochondria-containing species by successive loss of mitochondrial genes and its typical functions [29], with the notable exception of [Fe-S] protein biogenesis [30,31]. These findings suggest that the role of these organelles lies in the maturation of [Fe-S] proteins, which are known to be involved e.g. in DNA synthesis and repair [32, 33], ribosome assembly [34], translation initiation [35] or telomere length regulation [36]. The essentiality of many [Fe-S] proteins sharply contrasts with the importance of other mitochondrial processes such as ATP synthesis, citric acid cycle, and fatty acid oxidation which can be, under certain conditions, deleted in yeast without loss of cell viability. Thus it is rather the involvement in [Fe-S] protein biogenesis that makes mitochondria and its evolutionary reduced forms indispensable for life [37].

### 1. 2. 1. Iron sulphur cluster protein biogenesis in mitochondria:

### The ISC-assembly machinery

Please note that in the following text we use yeast nomenclature of protein titles, homologues of identical functions are however known in other organisms (for a list of names of the human homologues see Fig. 2).

As noted above, the basic principle of [Fe-S] protein biogenesis is the *de novo* synthesis of an [Fe-S] on a so called scaffold protein (see Fig.1). This step as well as the final transfer to the target apoproteins requires the aid of additional helper proteins [13]. The scaffold proteins are among the most conserved proteins of all [Fe-S] assembly factors, and they contain three conserved cysteine residues crucial for their function [38]. Molecular mechanisms of the release of the cluster from the scaffold protein, its conversion to other types of clusters and the incorporation into the apoproteins have yet to be defined. A number of proteins represent candidates for assisting these steps [23].

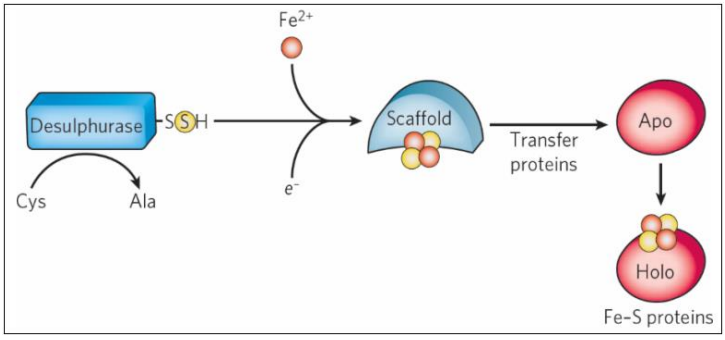


Fig.1: Basic steps of Fe-S cluster assembly and [Fe-S] protein maturation [39].

The sulphur atom required for the cluster assembly is released from a cysteine residue of a sulphur donor protein by the cysteine desulphurase ScNfs1 (IscS/NifS/SufS in prokaryotes), which attacks the sulfhydryl group (-SH) leading to the formation of alanine and a persulfide group (-SSH) which remains bound to the conserved cysteine residue of the enzyme (see Fig.2) [40]. In prokaryotes the sulphur is then directly transferred to the scaffold protein IscU [16], for which it was shown that both [2Fe-2S] and [4Fe-4S] clusters can be sequentially assembled and then transferred to appropriate apoproteins [41]. In eukaryotes the protein ScIsd11 is additionally needed to form a complex with ScNfs1 to enable the transfer of sulphur atom to the scaffold protein complex ScIsu1/ScIsu2. The particular function of ScIsd11 is not yet clear, however it has been demonstrated to be indispensable for the formation of [Fe-S]s [42].

Iron is taken up by mitochondria in its reduced form ($Fe^{2+}$), the import process demands an energized inner membrane [43], and possibly the mitochondrial carrier proteins ScMrs3 and ScMrs4 [44]. The iron atom is then delivered to the scaffold proteins by

ferroxidase ScYfh1 (see Fig.2). Ferroxidase is an enzyme able to bind iron ions and catalyse their oxidation ($Fe^{2+} \rightarrow Fe^{3+}$), and it is also known to interact with the scaffold proteins [45].

Subsequently an electron transfer chain is activated. Electrons are gained from the oxidation of NAD(P)H and are (assumed to be) transferred to the sulphur ($S^{-1}$) formed by the cysteine desulphurase reaction to generate sulfide ($S^{2-}$) required for the generation of an [Fe-S] [12, 13, 18, 45]. The electron transfer calls for a number of protein interactions, many proteins representing candidates for assisting in this step have been identified. ScYah1 has recently been characterised as a central player in this process, as its depletion results in a drastic decrease of *de novo* assembly of the mitochondrial [Fe-S] proteins [46]. By analogy to the well studied human adrenodoxin (FDX1), ScYah1 is predicted to receive electrons from the NAD(P)H-dependent adrenodoxin-reductase (FDXR) homologue ScArh1 (see Fig. 2). The target of the electron transfer however is unknown. Furthermore the proteins mentioned probably perform additional tasks in heme synthesis and iron storage [47] and may also take part in later steps of [Fe-S] protein biogenesis (e.g. in the dissociation of an [Fe-S] from the scaffold protein). But still the experimental evidence for this idea is lacking, and the chemistry behind an [Fe-S] formation on the scaffold protein is far from being understood [12].

To transfer the pre-assembled cluster from the scaffold protein to a transfer protein which targets it into the recipient apoprotein, chaperon proteins of the Hsp70 family (ScSsq1/ScJac1) are needed [48]. The latter protein (ScJac1) targets the former (ScSsq1) to the highly conserved binding motive (Leu-Pro-Pro-Val-Lys) present on the scaffold proteins [50] and, consequently, cycles of ATP binding and hydrolysis (ScSsq1 possess an ATPase activity, which is stimulated by ScJac1) lead to conformational change of the scaffold complex, thereby releasing the [Fe-S] [49]. In eukaryotes constituents of the complex (ScIsu1/ScIsu2, ScSsq1) may be recycled by the nucleotide exchange factor ScMge1 (see Fig. 2) [51]. The precise function of the chaperones in this process remains enigmatic, they are suggested to facilitate the transfer of an [Fe-S], stabilize conformation of the scaffold protein or regenerate it for the next round of the cluster assembly. The released [Fe-S] is then passed on to a transfer protein or directly to apoproteins. Specific interactions between chaperone and an apoprotein cannot be excluded but have not yet been reported [12].

The glutathione-dependent oxidoreductase (ScGrx5) possibly serves as an [Fe-S] transfer protein, as it has been shown to specifically interact with the chaperone subunit ScSsq1 [48]. The direct delivery of the clusters to apoproteins via ScGrx5 seems possible, the exact function is not known, nevertheless depletion in yeast resulted in the accumulation

of [Fe-S]s on the scaffold protein, and consequent defects in cytosolic [Fe-S] protein assembly [52].

The final component of the ISC-assembly machinery is a protein (ScNfu1) which shows targeting specificity, and was reported to bind [4Fe-4S], and so it is anticipated to transfer the cluster to the target apoproteins (see Fig. 2) [18]. Moreover ScNfu1 may be a potential interaction partner of the chaperones of Hsp70 family [23]. Apart from mitochondria, small amounts of ScNfu1 were also found to be localized to the nucleus and cytosol, thus the protein may participate in mitochondrial ISC assembly machinery as well as in cytosolic and nuclear [Fe-S] protein maturation, no functional data are however currently available to examine this hypothesis [13].

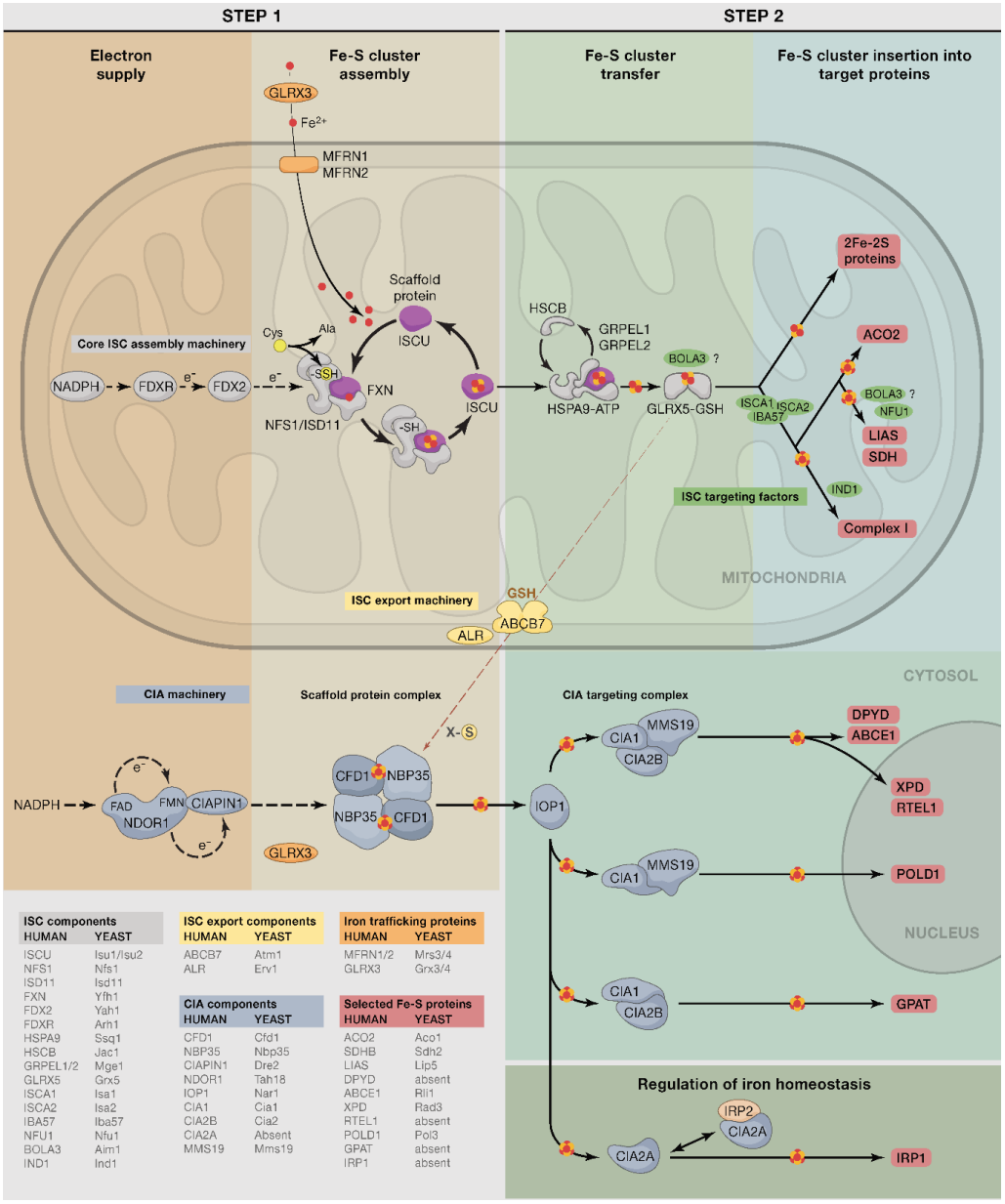


Fig. 2: Overview of the [Fe-S] protein biogenesis pathways in eukaryotes [53].

### 1. 2. 2. Iron sulphur cluster protein biogenesis in cytosol and nucleus: ISC-export machinery & cytosolic iron sulphur cluster-assembly (CIA) machinery

Since a product of the mitochondrial ISC-assembly machinery - the unknown sulphur containing compound - participates in the formation of [Fe-S]s outside the organelle [54, 14], an ISC-export machinery is established [12, 13]. The sulphur moiety needed for the incorporation into [Fe-S]s in cytosol is produced by the mitochondrial cysteine desulphurase exclusively, and thus the cysteine desulphurase (ScNfs1), the scaffold protein (ScIsu1/ScIsu2) and members of the ISC-export machinery were shown to be essential for [Fe-S] protein maturation outside the organelle [24, 59].

An ABC transporter (ScAtm1) localized in the mitochondrial inner membrane was the first protein identified to have specific function in cytosolic [Fe-S] protein biogenesis, as depletion of ScAtm1 resulted in leucine auxotrophy, since leucine biosynthesis is assisted by 3-isopropylmalate isomerase Leu1, a cytosolic [Fe-S] enzyme [24, 55]. These findings indicated that the ABC transporter exports the component needed for [Fe-S] protein assembly in the cytosol (see Fig. 2). The molecular nature of the substrate of the transporter is not clear, though the ATPase activity of the transporter is known to be stimulated by compounds containing sulfhydryl groups, and in particular by peptides with multiple cysteine residues [56]. The crystal structures of both ScAtm1 and related bacterial ABC transporter shows that the transporter possess substrate binding pocket comprised of a large, positively charged cavity which is able to bind glutathione (GSH), the cavity however provides much more space than for GSH alone, thus it is probable that GSH is a part of larger ScAtm1 substrate. GSH similar to ScAtm1 is also essential for extra-mitochondrial [Fe-S] protein maturation, and thus may also be directly involved in the export reaction [57]. Hence the available information suggest that the ISC-assembly machinery produces a component which is, after appropriate stabilization, exported via the ABC transporter to be used in the formation of cytosolic and nuclear [Fe-S]s.

The sulfhydryl oxidase (ScErv1) which is located in the mitochondrial intermembrane space (IMS) is naturally required for the oxidation of sulfhydryl groups in the IMS (see Fig. 2), and so it may facilitate the export of the unknown compound, e.g. by the introduction of disulfide bridges, and thus stabilize the compound before further transport into the cytosol [14]. Additionally in conjunction with ScMia40, ScErv1 takes part in disulfide-formation-driven import of cysteine-rich protein precursors into the IMS by oxidizing thiol residues, whereby coupling the process of translocation to oxidative folding.

The electrons released (from both of these sulfhydryl oxidation processes) may be delivered by the enzyme either to molecular oxygen or to cytochrome c, the latter considered to be the preferred electron acceptor *in vivo* [58].

The tripeptide glutathione (GSH) is thought to be involved in the ISC-export machinery (see Fig.2), as its depletion results in severe defects in cytosolic and nuclear, but not in mitochondrial [Fe-S] protein biogenesis [59]. Precise function is not yet clear, however other components of the ISC-export machinery tend to act in GSH-dependent fashion (as noted above). GSH was reported to be able to coordinate and stabilize [2Fe-2S] and to form cluster-bridging dimers with glutaredoxines (ScGrx), suggesting that a tetra-GSH-coordinated [2Fe-2S] may be an attractive substrate for ScAtm1. Further GSH is known to serve as redox-buffering agent and to take part in post-translational modifications, consequently affecting cell signaling pathways, ion channel activity and protein folding [60].

All compounds of the ISC-export machinery are highly conserved, and thus homologous in sequence and function. Therefore human homologues are able to restore phenotypic defects in yeast mutants [61], and ScAtm1 can even be replaced by plant homologues [62].

Components of the cytosolic [Fe-S] assembly **(**CIA) machinery are involved in the maturation of cytosolic and nuclear [Fe-S] proteins exclusively (see Fig. 2). The P-loop NTPases (ScCfd1, ScNbp35) are known to form hetero-tetrameric complex, serving as a scaffold for the assembly of [4Fe-4S] clusters. It is currently unknown, whether the CIA machinery is also capable of assembling [2Fe-2S] clusters or if there might be other cytosolic assembly pathways established for those. The source of sulphur for the CIA machinery is provided by the mitochondrial ISC-assembly machinery, as noted above. The source of iron stays for debate, possibly monothiol glutaredoxins (ScGrx3, ScGrx4) could be involved in the delivery of either iron or an [Fe-S] to the scaffold complex, as depletion of these proteins resulted in a defective insertion of iron into the apoproteins. The electrons for the cluster assembly are provided via the NAD(P)H –dependent electron transport chain composed of ScTah18 and ScDre2. The newly synthesized cluster is transferred from ScCfd1-ScNbp35 by ScNar1 to the CIA targeting complex consisting of ScCia1, ScCia2 and ScMms19. The CIA targeting complex then transfers the assembled [Fe-S] to cytosolic [Fe-S] apoproteins [63].

### 1. 3. MIA pathway

Biogenesis of proteins in general requires folding of the newly synthesized polypeptide chains which proceeds in prokaryotes in the periplasmatic space, and in eukaryotes in the endoplasmic reticulum and in the IMS of mitochondria. The final three dimensional structures of proteins are often stabilized by oxidation of two cysteine residues within the incoming polypeptides, thus creating a disulfide bond. Since spontaneous oxidation of thiol groups would be inefficient *in vivo*, protein machineries are established to catalyze this process. A broad range of enzymes and chaperones are required for folding of their client proteins in an energy-dependent manner [64]. Proteins providing oxidation of substrates become reduced and thus need to be reoxidized.

Since the components of the mitochondrial proteome are mostly nuclear encoded (especially when it comes to the IMS of mitochondria [58]), and synthesized in the cytosol [65], various import and assembly machineries have been developed to enable specific targeting and integration of every single protein into one of the four mitochondrial subcompartments - the outer membrane, IMS, inner membrane or the matrix. The Translocase of the Outer Membrane (TOM complex) is frequently referred as to the "common entry gate". Upon passage, protein-precursors are directed to defined biogenesis pathways by the interplay between specific sorting signals and the translocation machineries (see Fig. 3) [64].

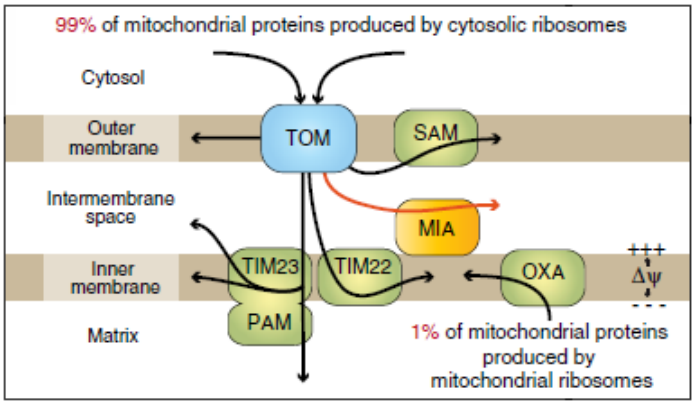


Fig. 3: Overview of mitochondrial import pathways [64].

Protein-precursors displaying beta barrel structure are subsequently recognized by the Sorting and Assembly Machinery (SAM complex) to mediate insertion and assembly into functional complexes of the outer membrane. Precursors directed to the inner membrane are guided by multiple non-cleavable internal targeting signals, which usually overlap with their hydrophobic transmembrane segments. Such polypeptides then tend to the Carrier Translocase (TIM22 complex) to be integrated into the inner membrane. Protein-precursors

targeted to the mitochondrial matrix typically carry a positively charged N-terminal signalpeptide leading them to the Translocase of the Inner Mitochondrial Membrane (TIM23 complex). Upon the translocation, the Presequence Translocase Associated Motor (PAM complex) is further required for the proteolytic cleavage of the pre-sequence, and consequently, the protein is folded into an active conformation with the aid of chaperones of the Hsp70 family [64].

Many proteins of outstanding importance are localized to the IMS e.g. components of the electron transport chain, enzymes, transporters, apoptotic factors. Whereas their physiological function was examined thoroughly, little is known about their biogenesis. The mitochondrial inermembrane space assembly pathway, in contrast to all the other mitochondrial import pathways mentioned, proceeds without the need for either inner membrane potential or hydrolysis of ATP in the mitochondrial matrix [64].

IMS-targeted protein-precursors of molar mass higher than 20kDa contain a bipartite signal, which consists of N-terminal matrix-targeting presequence and a hydrophobic sorting signal. So they first follow the presequence pathway governed by TIM23 and upon proteolytic removal of the presequence, mature soluble proteins are released into the IMS [64].

On the other hand, IMS-directed protein-precursors of small size (up to 20kDa), which contain conserved patterns of cysteine residues, are imported via the Mitochondrial IMS Assembly (MIA), also referred as to “mitochondrial disulfide relay”. The MIA machinery introduces disulfide bonds into the incoming precursors and thus couples the process of translocation to oxidative folding, consequently trapping the mature proteins in the IMS of mitochondria. Therefore the MIA pathway regulates structure, stability and function of a variety of proteins, whereby maintaining the integrity of the IMS. Therefore it is crucial for functional mitochondria and ultimately the entire cellular metabolism, in all eukaryotes [66].

In yeast there are two proteins of central importance which facilitate the process; ScMia40, which oxidizes the incoming substrates, and ScErv1 (“essential for respiration and vegetative growth”) which keeps ScMia40 in an oxidized state. ScErv1 is then reoxidized by cytochrome c which ultimately transports the electrons to the electron transport chain [67]. Both of the proteins (ScErv1, ScMia40) are essential for viability in yeast [68, 69].

As noted above, the substrates of the MIA pathway are proteins of small size located in the IMS. They contain conserved patterns of cysteine residues (see Fig. 4), which are involved in binding cofactors and in the formation of disulfide bonds [67], and thus the

cysteine residues are critical for the import and stable folding of these proteins. These patterns consist of one or several motifs of cysteine pairs spaced by either three ($CX_3C$) or nine ($CX_9C$) amino acid residues [70]. Upon oxidation, the proteins usually adopt a helix-loop-helix fold stabilized by two parallel disulfide bonds (see Fig. 4) [71]. Substrates of the $CX_3C$ family are small Tim chaperones required for the assembly of the TIM complex [67, 72], while the $CX_9C$ family harbours proteins of diverse functions, e.g. ScMia40, ScCox17 (taking part in the biogenesis of cytochrome c oxidase) or ScMdm35 (playing role in lipid homeostasis) [64]. Additionally there are two other proteins, which do not contain a $CX_3C$ nor a $CX_9C$ motif and still are imported via the MIA pathway, these are ScErv1 and ScCcs1 (copper chaperone involved in oxidative stress protection) [73, 74].

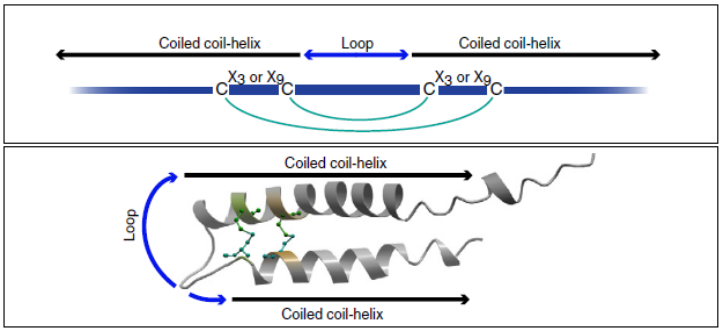


Fig. 4: Structure of the substrates of MIA pathway [64].

Recognition and binding of substrates is provided, beside the target cysteine residue, by a specific nine amino acid sequence upstream or downstream of the docking cysteine, altogether termed IMS-targeting signal (ITS), so the interactions with Mia40 are both covalent and hydrophobic [75].

It is not yet clear whether the MIA-driven import takes its course in a post- or co-translational manner, since both were shown to be functional *in organello* [76-78]. Many substrate proteins however are not of sufficient length to span the ribosome and the outer mitochondrial membrane in such way that the ITS is available for the interaction with ScMia40 in the IMS and, furthermore the ITS is not always located on the N-terminus of the substrate protein [75].

ScMia40 is anchored to the mitochondrial inner membrane via the hydrophobic N-terminus, while a large domain is exposed into the IMS, displaying six conserved cysteine residues arranged in a CPC and a twin $CX_9C$ motif (see Fig. 5). The CPC motif in its oxidized state enables ScMia40 to interact with reduced substrates via the intermolecular disulfide bonds [79]. Under steady-state conditions about 80% of ScMia40 is present in its oxidized, active form, and when levels of ScErv1 are down-regulated, ScMia40 is shifted to its reduced form [58]. Depletion of ScMia40 results in the inhibition of import of cysteine-

rich IMS members, while other mitochondrial import pathways were reported to be unaffected [64].

ScMia40 i) functions as a receptor, that can recognize the ITS signal and transiently interact with the incoming polypeptides via disulfide bonded intermediates (negotiated by ScMia40's redox-active CPC motif) [75, 80] and, ii) serves as an oxidoreductase and a chaperone, as upon the formation of the intermediate, disulfide bonds are transferred to the substrate in the process of oxidative protein folding (see Fig. 6) [81]. The substrate protein is thus converted from its reduced import-competent state to an oxidized, stably folded protein, which cannot transverse back out of mitochondria. It is not yet clear, whether the oxidizing equivalents are coming from a ScMia40 mono- or dimer or from ScErv1, however the presence of ScErv1 increases the efficiency in the transfer of multiple disulfide bonds [82].

The translocation process is further influenced by physiological glutathione (GSH) concentrations. An accelerating effect of GSH on the electron flow through the disulfide relay to cyt c was observed. Moreover GSH prevents the formation of a partially oxidized intermediates, and protects the oxidized substrates and the electron transfer between ScMia40 and ScErv1 from reduction [83]. Upon the formation of intramolecular disulfide bonds within the substrate, the interaction between the substrate and ScMia40 is terminated, and ScMia40 is released with a reduced CPC motif [84]. ScErv1 participates in recycling ScMia40 by reoxidizing its cysteine residues, the electrons are then transferred probably via cyt c to the respiratory chain where they are ultimately passed on to molecular oxygen [58].

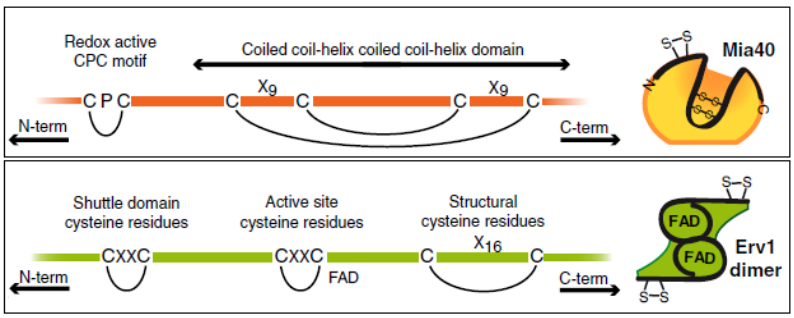


Fig. 5: Structure of ScMia40 and ScErv1 [64].

ScErv1 is a FAD-linked oxidoreductase, that displays two pairs of redox-active cysteines (arranged in CXXC motif); the N-terminal pair forms a catalytic domain which mediates the electron transfer from ScMia40, the second pair (situated on the C-terminus, adjacent to the FAD-binding domain) is required for the generation of the first one and is than reoxidized by FAD. A third pair of conserved cysteine residues is arranged in a $CX_9C$ motif and serves a structural role, as these are responsible for the non-covalent dimerization of ScErv1(see Fig. 5). The homodimer is thus able to shuttle electrons from ScMia40 via the

N-terminus onto the FAD domain by intersubunit electron transfer, and finally the electrons are transferred from the FAD domain to cyt c (see Fig. 6). Therefore both domains are essential for the function, even thought only the N-terminal one directly interacts with ScMia40 [85].

Lack of ScErv1 is reported to cause aberrant mitochondrial morphology, loss of mitochondrial DNA, respiration defects and defects in cytosolic [Fe-S] proteins biogenesis [86, 87]. Depletion of ScErv1 prevents the import of cysteine-rich IMS proteins, as the precursors remain associated with ScMia40, and its absence is therefore lethal for the cells [65].

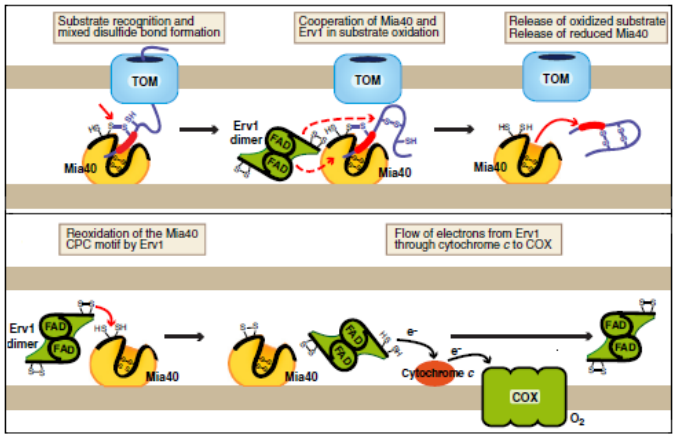


Fig. 6: MIA reaction cycle [64].

Upon the reoxidation of ScMia40 by ScErv1, the electrons released are passed to an electron acceptor, so that ScErv1 is also recycled to an oxidized state. Sulfhydryl oxidases such as ScErv1 are generally predicted to use oxygen as an electron acceptor [88]. During this process hydrogen peroxide ($H_2O_2$) is generated and subsequently reduced to water by cytochrome c-peroxidase (ScCcp1). ScCcp1 is then in turn reduced by cyt c [89]. Such mechanism is utilized by the sulfhydryl oxidase of the endoplasmic reticulum (ScEro1) [90]. However it has been shown both *in vitro* [91] and *in organello* [89] that ScErv1 as well as the human homologue (ALR), can transfer electrons also directly to cyt c, thus increasing the efficiency by which both compounds are reoxidized and, preventing the generation of potentially harmful reactive oxygen species [58]. Cyt c can then be reoxidized using a variety of pathways, including the electron transport chain or ScCcp1 [89]. For the human homologue of ScErv1 (ALR), cyt c was shown *in vitro* to be a 100-fold more effective electron acceptor in comparison to oxygen [91]. Moreover ScErv1 was reported to form a high affinity complex with cyt c and also to be able to directly reduce the heme of cyt c [89].

*In vitro* cyt c can accept electrons from a variety of sulfhydryl oxidases, including those that are not present in the mitochondria. Since both ScErv1 and cyt c reside in the IMS, their interaction is feasible and physiologically reasonable and may additionally prevent the

cell from the oxidative damage [58]. Hence cyt c is considered to be the preferred electron acceptor for Erv1 in yeast and mammals [58, 89].

Interestingly, *S. cerevisae* possesses two genes for cyt c, which are differentially expressed under high and low oxygen concentrations [92], so that different forms may function in different environmental conditions. Also Erv1 may display a level of flexibility, since both ScCcp1 and cyt c are synergistic with ScErv1, both noticed pathways may occur simultaneously, so Erv1 may shuttle electrons both to oxygen and to cyt c [89].

### 1. 3. 1. MIA pathway in Kinetoplastida

As it has already been mentioned, mitochondrial genomes are usually greatly reduced, and are coding only for a minor portion of the total proteome that constitute the organelle, therefore most proteins are targeted into mitochondria post-translationally [65], and so the mitochondrial protein import (MPI) pathways are essential for the biogenesis of mitochondria in all eukaryotes [93]. As the mitochondrial endosymbiosis only occurred once in the evolution, many features of the mitochondrial biology tend to be conserved even among distant phylogenetic lineages [94, 95]. Regarding the import pathways into the organelle, it is observed that the channel-forming subunits of integral membrane protein complexes are usually well conserved, whereas other components of the import apparatus may vary significantly [96]. Studies indicate that the MPI pathways are functionally conserved among all eukaryotes despite compositional differences of the machineries [93].

Notably regarding the MPI pathways in Trypanosomes, some anomalies were reported previously, e.g. the TOM complex is yet to be defined, mitochondria-targeting sequences are much shorter compared to other eukaryotes, moreover there is only a single translocase of the inner membrane which facilitates both translocation across the membrane and protein insertion into the membrane [97].

The import into the mitochondrial IMS is achieved via the mitochondrial IMS assembly (MIA) machinery which, in yeast, consists of ScMia40 and ScErv1 as noted above. The MIA pathway as described for animals and yeast is however not conserved in several protist lineages, including apicomplexan and kinetoplastid parasites. These organisms seem to lack a Mia40 homologue although the substrates for Mia40-dependent import are present, and thus they most probably possess altered import machineries [93, 98]. In contrast Erv1 seems to be conserved among virtually all eukaryotes [87], which raises the question about how the cysteine-rich proteins are imported into the IMS in the organisms lacking a Mia40

homologue and which exact role is Erv1 playing in mitochondrial import and/or export machineries.

Kinetoplastid genome sequences were previously analysed, and an Erv1 homologue as well as small Tims were identified, while no trace of a Mia40 homologue was reported. These findings suggest that the composition of the MPI machineries varies significantly from those known in human and yeast, insomuch that Mia40 was initially considered to be indispensable for the import of small cysteine-rich proteins into the IMS [68, 93, 98].

It has been shown *in vivo* and *in organello* that the import is functionally conserved, experiments were performed in *Leshmania tarentolae*, another representative of the class Kinetoplastida, and a model organism. It was demonstrated that *L. tarentolae* proteins of all four mitochondrial subcompartments are efficiently imported into isolated yeast mitochondria and similarly opisthokont marker proteins are successfully imported into isolated *L. tarentolae* mitochondria. Interestingly LtErv1 is imported into the IMS of yeast Mia40-depleted mitochondria, pointing to an alternative import mechanism, obviously independent of Mia40p. In spite of the successful import reaction the proteins however could not complement the function of each another (LtErv1 cannot complement knock-out of ScErv1), likely because of a different architecture of the proteins [93].

The study further revealed that kinetoplastid Erv1 homologues display altered cysteine pair motifs (see Fig. 7). All eukaryotic Erv1 homologues display the proximal (active-site) cysteine pair, adjacent to the flavin cofactor, that is the only cysteine pair conserved among all of the homologues, and was shown to be essential for the oxidase activity of ScErv1 [99] as well as TbErv1 [100]. And next, all homologues contain the distal (shuttle) cysteine pair, which tends to be variable, especially concerning the number of spacing residues, while in most opisthokonts it is arranged in a Cys-Arg-X-Cys motif located to the N terminus, kinetoplastida display the distal cysteine pair arranged in Cys-X-Val-Tyr-C motif located to the C terminus of the protein [101].

Additionally the special feature seen in kinetoplastid Erv1 homologues is an abnormally extended C terminal domain (see Fig. 7), which consists of some 200 amino acid residues, hence a term Kinetoplastida-specific second (KISS) domain was suggested [101]. Although this domain is present in Kinetoplastida ubiquitously, it is rather variable, as the sequences differ not only between *Leishmania* and *Trypanosome*, but also in between *Trypanosome* species [93].

Interestingly studies in plants stated that *Arabidopsis thaliana* Erv1 homologue shows similarities to that of trypanosome (see Fig. 7). In particular, while in most eukaryotes

the distal cysteine pair is spaced by two amino acid residues and the is motif located to the N terminus, AtErv1 homologue, similarly to TbErv1, display a $CX_4C$ motif at the C terminus of the protein (see Fig. 7). Furthermore the experiments revealed that, contrary to AtErv1, AtMia40 is not essential, as depletion of AtMia40 showed lack of phenotype and no significant effect on the MPI was observed. These results indicate that the mitochondrial disulfide relay system functions without AtMia40. Additionally the amount of AtErv1 in Mia40-depleted plants is significantly increased, suggesting that the different arrangement of cysteine pairs in AtErv1 and TbErv1 may allow Erv1 alone to function as a replacement of the MIA pathway [102].

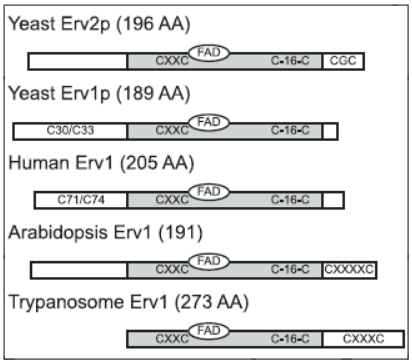

Fig. 7: Location of cysteine pairs in Erv1 homologues [102].

Deep evolutionary origins of Trypanosomes and other Excavata suggest that these "altered" MPI pathways could actually reflect the ancestral targeting pathways in the first eukaryotes, where the import into the mitochondrial IMS was possibly only dependent upon Erv1, not Mia40 [98]. The multi-functionality and ubiquity of Erv1 provides an argument for earlier origin of this protein. Furthermore ScErv1 is required for ScMia40 function, as Erv1-depleted yeast mitochondria allows the formation of Mia40-substrate disulfide intermediate but the release of the oxidized substrate is inhibited, consequently causing an accumulation of the reduced, inactive form of ScMia40 [103]. The idea is further supported by the fact that in organisms lacking an Erv1 homologue, substrates of the MIA pathway are not present [98]. Alternatively Erv1 may cooperate with an unknown component. Owning to lack of experimental data we can not discriminate between the different evolutionary scenarios yet.

### 1. 4. Role of Erv1 in *T. brucei*

In yeast and animals ScErv1 is known to function in conjuction with ScMia40 in the import of small cysteine-rich proteins into the IMS of mitochondria. Available data suggest that TbErv1 functions in protein import into the IMS despite the natural absence of a Mia40 homologue, as massive mitochondrial swelling is observed following TbErv1 gene silencing [100]. Mitochondrial swelling is known to be a common feature to defective MPI in yeast, and alterations in mitochondrial morphology were also shown to be associated with the knock-down of ScErv1 [86]. ScErv1 was additionally shown to cause impaired respiration, loss of mitochondrial genome, decreased amount of small cysteine-rich proteins in the mitochondrial IMS and accumulation of reduced, non-functional form of ScMia40 [103].

Further TbErv1 is believed to play a role in the export of an unknown compound produced by the ISC machinery, which is required for the maturation of cytosolic and nuclear [Fe-S] proteins, which are known to be involved in variety of essential cellular processes [100]. The idea is additionally supported by observations in other protists, e.g. *Encephalitozoon cuniculi* lacks a Mia40 homologue as well as substrates for the MIA pathway, still EcErv1 presumably functions in the cytosolic [Fe-S] assembly, since known components of the CIA machinery are conserved, further *Entamoeba histolytica* lacks an Erv1 homologue and its ISC machinery is replaced by Nif-like system. Moreover the loss of Erv1 in some organisms generally correlates with the absence of an Atm1 orthologue, thus driving the evolution of Atm1-independent mitochondrial [Fe-S] export system [98].

Regarding the physiological oxidant of TbErv1 one hypothesis suggests that in the procyclic form of *T. brucei* which rely on a functional respiratory chain, cytochrome c serves as the terminal electron acceptor. Electrons from the reduced cytochrome c would then probably be transferred to oxygen, as the cytochrome c peroxidase is absent from the genome of *T. brucei*. In contrary the bloodstream form of *T. brucei* has no capacity for respiration, but TbErv1 is still essential for the mitochondrial import and/or export. The hypothesis suggests that in bloodstream form TbErv1 is oxidized directly by oxygen. Since the activity of the sulfhydryl oxidase TbErv1 is likely to be low, any reactive oxygen species generated as by-products could be acted by parasite's antioxidant defence mechanisms [98].

As Trypanosomatids are of deep evolutionary origins, they may reflect the ancestral simplicity, which may be present, yet cryptic in higher eukaryotes, as in the course of evolution the cellular pathways gradually became more refined. Although the mitochondrial biology of *T. brucei* appears to have many unique features, previous studies demonstrated that many of the "unique" phenomena first discovered in Trypanosomes were subsequently

found to be general features of all eukaryotes (e.g. trans-splicing of nuclear RNA, RNA editing). We suppose this may also be true for some apparently "unique" aspects of the mitochondrial biology of *T. brucei*, thus the study of mitochondrial protein import may have further implications for the elucidation of these mechanisms in eukaryotes in general. Furthermore since mitochondrial protein import is expected to be essential for cell survival, the differences between Kinetoplastid Erv1 homologue and mammalian ALR might serve as starting point for drug development [97].

# 2. AIMS OF THE THESIS

1) To verify the subcellular localization of TbErv1.

2) To examine the role of TbErv1 in the iron-sulphur cluster protein biogenesis.

3) To search for possible interaction partners of TbErv1.

### 3. 1. Cell culture of *T. brucei*

Two different parental cell lines of procyclic *Trypanosoma brucei brucei* were used to perform the experiments. The RNAi cell line 29-13 [104], which is based on wild type *T. brucei brucei* Lister strain 427, the cell line SmOxP9 [105], which is based on wild type *T. brucei brucei* TREU927 [5] and an RNAi cell line for the knock-down of Erv1, constructed by Somsuvro Basu [100].

The cells were grown in SDM-79 medium supplemented with 10% fetal bovine serum at 27°C [106]. The cell line 29-13 was grown under the presence of the antibiotics hygromycin (50 µg/mL) and neomycin (15 µg/mL) [104]. Medium for the knock-down cell line was additionally supplemented with phleomycin (2.5 µg/mL), and for the induction of the RNA interference tetracycline (1 µg/mL) was added once per 24 hours. The cell line SmOxP9 was grown under the presence of the antibiotic puromycin (1 µg/mL).

Concentrations of cells were measured using a Z2 Coulter Particle Count and Size Analyzer (Beckman Coulter) (dilution factor=200, TI=3,5 µm, Tu=7,7µm, count=between).

### 3. 2. v5 tagging

#### 3. 2. 1. PCR-only tagging

» *Principle:* The Polymerase Chain Reaction (PCR) only tagging (pPOT) series of plasmids were designed to enable tagging of gene of interest in *T. brucei* at its endogenous locus. As trypanosomes only require 50 nucleotides of identity for targeted homologous recombination, it is possible to incorporate such sequence into long PCR primers. The plasmid contains a tag and a resistance gene, which can be amplified using the long primers that contain a short region of identity to the plasmid and a longer region (about 80 nucleotides) of homology to the gene locus to be tagged, which is thus incorporated into the plasmid. The amplicon is then used to transfect *T. brucei* and so it can recombine with the genomic DNA such that the tag is fused to the target gene [107].

Table 1: PCR programme.

| Temperature | Time | |
|---|---|---|
| 94°C | 5 min | |
| 94°C | 15 sec | |
| 60°C | 30 sec | |
| 72°C | 2 min | 2↑ 30 cycles |
| 72°C | 2 min | |
| 16°C | pause | |

Tab. 2: Materials used for PCR only tagging and PCR reaction mixtures.

| | | |
|---|---|---|
| Erv1 Forward primer | ctgaaacgaa aaaggacaag agggagggaa aacaaacaac gagaaaagat actttatcgt aggaactttc ctgactcaac gtataatgcagacctgctgc | |
| Erv1 Reverse primer | ataatccagc ctgccttacc cagttctcgg ggcgtcggac actcaccggg aatcttctgc aacggctcct gtttcgacat actacccgatcctgatcc | |
| pPOTv4 | [107] | |
| PCR Mixture A | DMSO (PCR grade) | 0.5 µL |
| | Forward Primer, 100 µM (final conc. 2 µM) | 1 µL |
| | Reverse Primer, 100 µM (final conc. 2 µM) | 1 µL |
| | 25 ng template (pPOTv4-v5, 25 ng/ µL stock) | 1 µL |
| | dNTPs, 10 mM each (final conc. 0.2 mM) | 1 µL |
| | MiliQ $H_2O$ | 44 µL |
| PCR Mixture B | Expand HiFi buffer 2 (Roche, 04 743 725 001) | 5 µL |
| | Expand HiFi polymerase (Roche, 04 743 725 001) | 1 µL |
| | MiliQ $H_2O$ | 19 µL |

» *Procedure*: Primers were designed according to the protocol for endogenous C-terminal tagging using the pPOTv4 plasmid [107]. For the PCR a modified pPOTv4 plasmid was used in which the YFP tag was replaced by 3x V5 tag, termed pPOTv4-v5. The DNA was amplified by PCR using a „Hotstart“ according to the published protocol [107] and upon analysis by agarose gel electrophoresis, the PCR reaction was used without further purification for the electroporation of procyclic *T. brucei*.

For the „Hotstart“ PCR, mixture A (according to Tab. 2) was placed into the thermocycler and the PCR program (see Tab. 1) was started. After the machine reached 94°C for 1 min, mixture B (according to Tab. 2) was added. When the reaction was completed, 5 µL of the reaction mixture were analysed by agarose gel electrophoresis to check for success of the reaction. One PCR reaction was performed without addition of the plasmid to serve as negative control (data not shown).

### 3. 2. 2. Agarose Gel Electrophoresis

» *Principle*: Agarose gel electrophoresis is a method used to separate DNA fragments by length by applying an electric field to move the charged molecules through an agarose matrix. Since DNA carries a negative charge on each of the phosphate groups making up its backbone, the DNA fragments migrate towards the positive electrode. As DNA molecules migrate, they are hindered by the meshwork of fibers that make up the gel. The larger molecules the harder it is for them to squeeze through the pores, conversely smaller molecules are able to move faster, and thus the result is that DNA fragments are separated according to their size. For visualization, the DNA gels are routinely stained with ethidium bromide, which intercalates in between the base pairs of DNA. When excited by UV light,

ethidium bromide bound to DNA fluorescence bright orange, which allows then to visualize the DNA present within the gel. To determine the size of a DNA fragment, a kilobase ladder is used, which is a set of standard DNA fragments of known sizes which is run alongside the gel and acts as reference [108].

Tab. 3: Chemicals used for Agarose Gel Electrophoresis.

| | |
|---|---|
| Agarose | 0,75% Agarose in 1x Agarose gel electrophoresis buffer |
| Ethidium bromide solution | 0,1 µg/mL Ethidium bromide in MiliQ $H_2O$ |
| 10x Agarose gel electrophoresis buffer | 670 mM Tris-Base, 222 mM boric acid, 5 mM EDTA |
| 6x MassRuler$^{TM}$ DNA Loading Dye | 10 mM Tris-HCl (pH 7,6), 0,03% bromphenol blue, 60% glycerol, 60 mM EDTA |
| 1kb DNA Ladder | (Invitrogen) |

» *Procedure:* 5 µL of the PCR reaction mixture was mixed with 1 µL of the Loading Dye and was run along with 7 µL of the 1kb DNA Ladder at 70V on a 0,75% agarose gel, until completed. For later visualization of the DNA 1 µL of the EtBr solution was added per 50 mL of the agarose gel, prior to casting. The results were visualized by exposing the gel to UV light on an Alphaimager® (HP systems).

### 3. 2. 3. Electroporation of procyclic *T. brucei*

» *Principle:* Electroporation is a technique for transfecting cells in suspension by applying an electrical pulse. The application of the electrical field induce the formation of pores within the cell membrane, thus increasing its permeability and allowing the DNA to be transformed to enter the cell [108].

» *Procedure:* The cell line SmOxP9 was grown in SDM-79 medium with appropriate drugs in concentrations between 0.5-1x$10^7$ cells/mL. 1x$10^7$ cells were harvested by centrifugation at 800 g, at RT for 10 min. The cell pellet was resuspended in 400 µL Cytomix (25 mM HEPES, 120 mM KCl, 0.15 mM $CaCl_2$, 10 mM $K_2HPO_4/KH_2PO_4$, 2 mM EDTA, 6 mM Glucose, 5 mM $MgCl_2$, pH 7.6) and 45 µL of the PCR reaction mixture was added. The resulting cell suspension mixture was then loaded into a 0.2 cm gap electroporation cuvette and electroporated with one pulse (1600 V, 25 Ω and 50 µF) on a BTX ECM650 Electro Cell Manipulator®. One electroporation was performed without the addition of the PCR reaction mixture, serving as negative control. The cell suspension was incubated with 9.5 mL fresh SDM-79 containing puromycin (1 µg/mL) at 27°C over night. When the cells thus recovered from the electroporation 20 mL of fresh media containing puromycin were added and additionally hygromycin was added to a final concentration of 100 µg/mL, serving as the selection marker. The cell suspension was then evenly divided into a 24 well plate. After 10-12 days, when there were no living cells observed in the

negative control, positive wells were screened for the expression of the v5-tagged protein by performing Western Blot Analysis, using anti-v5 antibody. One positive clone was selected and grown in higher volume for further experiments.

### 3. 3. Erv1-RNAi cell line

» *Principle:* RNA interference (RNAi) is a technique of gene silencing deriving benefit from the natural cell defence mechanisms against viruses. The RNAi is triggered by the introduction of a double stranded (ds) RNA, which is fully homologous to the gene of interest. As under normal circumstances dsRNA does not occur within the cell, it is recognized as foreign and thus cleaved into fragments of short interfering (si) RNAs by a nuclease known as Dicer. Subsequently siRNAs are bound and separated into single-stranded (ss) RNAs by the RNA-induced silencing complex (RISC), which is also displaying nuclease activity and thus is able to recognize and degrade any ssRNA corresponding in sequence to the bound siRNA. Thereby the transcripts of the gene of interest are eliminated [108].

Several methods of RNAi have evolved over time, including short hairpin (sh) RNAs capable of DNA integration. The shRNAs are synthesized within the cell upon introduction of a vector encoding for shRNA (homologous to the gene of interest) transcribed by an inducible promoter. Once transcribed, the shRNAs are exported to cytosol where they are recognized by the Dicer and thus follows the RNAi pathway. This method allowed us for stabile time-dependent regulation of gene expression [109].

#### 3. 3. 1. Growth curve

» *Principle:* The gene of interest is silenced via induction of the RNAi cell line by tetracycline, so that in case of essentiality of the gene of interest an influence on the growth rate can be observed.

» *Procedure:* Cells were grown in 1ml volumes of SDM-79 medium containing appropriate antibiotics with a starting concentration of $1x10^6$ cells/ml. Cell densities were measured every 24 hours and diluted back to the concentration of $1x10^6$ cells/ml. Gene silencing was induced for ten days by addition of fresh tetracycline to the culture media (1µg Tet/1ml media) once per 24 hours. The growth rate of induced cells was compared to that of the parental cell line (29-13) and non-induced RNAi cell lines, growth phenotype was observed. Calculation was performed using Microsoft Excel.

### 3. 3. 2. Aconitase activity measurement

» *Principle:* Aconitase is a known iron-sulphur cluster protein of two forms, the mitochondrial form acts as an enzyme of tricarboxylic acid cycle, which catalyses the conversion of citrate into isocitrate. The cytosolic form of aconitase provides isocitrate for other synthetic purposes and additionally, in mammals acts as iron regulatory protein [110]. In the genome of Trypanosomes, aconitase is encoded by a single gene while the protein is of dual localization. The [Fe-S] required for the activity of the enzyme is supplied by the respective [Fe-S] assembly machineries, so by ISC in mitochondria, and by CIA in cytosol [111]. When a gene of interest is silenced, the possible influence of its product on each of the [Fe-S] assembly machineries can be tested by the measurement of aconitase activity in mitochondria and cytosol independently.

Enzyme activities are determined by the measurement of moles of product formed by an enzyme in a given amount of time under given conditions per milligram of total proteins. The concentration of the product as well as the total amount of proteins can be determined using spectrophotometric methods. [112].

Tab. 4: Chemicals used for aconitase activity measurement.

| | |
|---|---|
| Lysis buffer | 25 mM Tris-HCl, pH 7.6, 225 mM Sucrose, 2 mM EDTA, 2 mM EDTA, 2 mM EGTA, 10 mM $KH_2PO_4$, 1 mM $MgSO_4$, 10 mM Na-Citrate, 2 mM Dithiotreitol (DTT), + cOmplete™, EDTA free protein inhibitor (1 tablet per 10 mL buffer) |
| Digitonin solution | 10 mg/mL digitonin in MiliQ $H_2O$ |
| Triton X-100 | 10% TX-100 in MiliQ $H_2O$ |
| 1x PBS | 137 mM NaCl, 2.7 mM KCl, 4.3 mM $Na_2HPO_4$, 1.47 mM $KH_2PO_4$, pH 7.4 |
| Activity buffer | 90 mM Tris, pH 7.5 |
| DL-isocitric acid solution | 0.5 M DL-isocitric acid trisodium salt in MiliQ $H_2O$ |

» *Procedure:* The cell lines 29-13 and Erv1-RNAi were grown in 100ml volumes of SDM-79 medium with appropriate drugs in concentrations between 0.5-1x$10^7$ cells/mL. The RNAi cell line was induced for 0, 2 and 4 days. 5 x$10^8$ cells of 29-13, non-induced and each day of induction for the RNAi cell line were harvested by centrifugation at 1000 g, at 4°C for 10 min.

The cell pellet was washed twice with PBS and sequentially resuspended in 500 µL of the ice-cold lysis buffer. This cell suspension was incubated on ice until use. 400 µL of the cell suspension were mixed with digitonin to obtain a final concentration of 0.4 mg/mL digitonin. The suspension was then vortexed for a couple of seconds and incubated at RT for 5 min. Upon centrifugation at 14 000 g, at RT for 2 min, the supernatant representing the cytosolic cellular fraction was collected and immediately placed on ice for later use.

The pellet was washed once with lysis buffer and sequentially resuspended in 400 µL of fresh lysis buffer, Triton X-100 was then added to a final concentration of 0.1% Triton X-100 and the mixture was incubated for 5 min on ice. This fraction represented the mitochondrial fraction.

100 µL of the remaining cell suspension were washed once with PBS and resuspended in 500 µL MiliQ $H_2O$. 10 µL of this suspension was then used to determine the total protein concentration via the Bradford protein assay.

For the aconitase activity measurement 10 µL of the lysate of each fraction were mixed together with 235 µL of the activity buffer and 5 µL 0.5 M DL-isocitric acid solution, representing the substrate. Samples of mitochondrial and cytosolic fractions were measured separately. Three replicas for each of the reactions were prepared (to avoid fluctuations by pipetting error) in a 96 well plate with UV transmissible bottom. The absorbance ($A_{240}$) was measured in 30 sec intervals over a period of 10 min, using Infinite® M200 PRO (Tecan). The rise in the absorbance corresponds to an increasing concentration of the product of the reaction (as stated by the Beer-Lambert law), which was used to determine the activity of cytosolic and mitochondrial aconitase respectively. The rise of absorbance was normalized to the total protein concentration, which was determined by the Bradford assay of the whole cells. Activities of induced cells were compared relative to non-induced. The aconitase activity measurement was performed in three independent repeats, and the three obtained values for each activity were used to calculate the confidence interval with a confidence level of 95%. Calculation was performed using Microsoft Excel.

### 3. 3. 3. Membrane Potential Measurement

» *Principle:* Mitochondrial membrane potential, *in situ*, is an important physiological parameter related to the capacity of the cell to generate ATP, and thus it is an indicator of mitochondrial function or dysfunction, which can then predicate about the cell health or injury. Changes in mitochondrial membrane potential ($\Delta\psi_m$) can be monitored using various fluorescent dyes, one of many possibilities is the MitoTracker Red CMXRos. MitoTracker Red is a cationic dye for staining mitochondria in living cells, and so it accumulates into the mitochondrial matrix in an inverse proportion to the to the mitochondrial membrane potential (more polarized mitochondria, with more negative interior, will accumulate more dye than a depolarized mitochondria) [113]. We have adopted a flow cytometry method for the quantitative measurement of $\Delta\psi_m$ which utilizes the cationic fluorescent dye MitoTracker Red. The method provides estimates of the $\Delta\psi_m$ *in situ*, in a heterogenous cell population,

since only the fluorescence of the cell bound dye is measured and the $\Delta\psi_m$ is estimated from the intensity of the cell fluorescence [114].

» *Procedure*: Cells were grown in SDM-79 medium with appropriate drugs in concentrations between 0.5-1x$10^7$ cells/mL. The RNAi cell line was induced for 0, 2 and 4 days, 1x$10^7$ cells of each of the cultures were incubated at 27°C with MitoTracker ® Red CMXRos at a final concentration of 200 nM for 30 min. Cells were harvested at 600 g, at RT for 10 min, the cell pellet was resuspended in 1 ml of IsoFlow™ Sheath Fluid. 100 µl of the cell suspension were mixed with 1 ml IsoFlow™ Sheath Fluid and thus prepared samples were then used for analysis by flow cytometry, which was carried out on BD FACSCantoII (BD Biosciences, USA). Calucation was performed using Microsoft Excel.

### 3. 4. Localization

Two independent approaches were used to determine the subcellular localization of TbErv1. Once a microscopy technique was utilized to detect the protein in its native position in fixed cells, and next a chemical fractination method was employed to separate the cellular compartments and allow the detection of the protein in the generated fractions.

#### 3. 4. 1. Immunofluorescence assay (IFA)

» *Principle:* IFA is an immunohistochemistry technique, usually used for visualization of structures at subcellular level. Therefore the method is limited to fixed cells, since cellular membranes first have to be permeabilized to allow the penetration of antibodies or other agents used for staining. The application of some fixatives may alter the tissue or even cause cross-linking of proteins, consequently leading to false results due to non-specific binding and generation of artefacts. On the other hand, apart from staining specific structures, the fixation also allows us to prepare permanent specimens, which can be re-analysed.

The basis of the technique lies in the specificity of the antigen-antibody interaction. While the primary antibody specifically binds to the protein of interest, it is sequentially recognized by the secondary antibody, carrying the fluorophore. As multiple secondary antibodies can be bound to a single molecule of the primary antibody, the fluorescent signal is thus amplified by increasing the number of fluorophore molecules per molecule of the antigen.When examined under the fluorescent microscope, the fluorophore is, upon light excitation, capable of re-emitting the light. The absorption (excitation) and emission spectra are specific to each fluorophore, the excitation energies are in general ranging from UV to visible spectrum, while emission energies continue from visible light to near infra-red region.

Thereby the method allows us to determine the distribution of the protein of interest within the cell [115].

Tab. 5: Materials and antibodies used for the immunofluorescence assay.

| | |
|---|---|
| MitoTracker® Red CMXRos | (ThermoFisher Scientific) |
| 4% paraformaldehyde | 1x PBS, 1,25 mM NaOH |
| Superfrost® plus slides | (ThermoFisher Scientific) |
| 1x PBS | 137 mM NaCl, 2.7 mM KCl, 4.3 mM $Na_2HPO_4$, 1.47 mM $KH_2PO_4$, pH 7.4 |
| 0.2% Triton X-100 | TX-100, 1x PBS |
| Methanol | |
| 5% milk | Dissolved in 1x PBS-Tween |
| ProLong® Gold Antifade reagent with DAPI | (molecular probes, P36935) |
| **Antibodies:** | |
| Anti-Erv1 | [100] |
| Anti-Hsp70 | [116] |
| Goat Anti-Mouse IgG H&L, Alexa Fluor® 488 | (Invitrogen) |
| Goat Anti-Rabbit IgG H&L, Alexa Fluor® 555 | (Invitrogen) |

» *Procedure:* The immunofluorescence assay was utilized for two purposes, first to determine the subcellular localization of TbErv1, using the SmOxP9 cell line, and second for the verification of prospective alterations in the mitochondrial morphology along with the gradual depletion of the protein, using the RNAi cell line. For the second, cells induced for 0, 2 and 4 days were used as the exemplary samples.

Cells were grown in SDM-79 medium with appropriate drugs in concentrations between 0.5-1x$10^7$ cells/mL. 1ml of SmOxP9 cell culture was incubated at 27°C with MitoTracker at a final concentration of 200 nM for 30 min. Cells were harvested at 1000 g, at RT for 2 min, the cell pellet was washed once with PBS and then resuspended in 200µL of 4% paraformaldehyde. The suspension was spread onto the slides and fixed for 20 min on air. The slide was then washed once with PBS and sequentially the cells were permeabilized with ice-cold methanol at -20°C for 20 min. For further permeabilization the cells were additionally incubated in 0.2% Triton X-100 for the next 20 min. The slides were washed once with PBS, blocked with 5% milk for 45 min at RT, and then incubated with the primary antibody for 2 hours at RT.

For the SmOxP9 cells polyclonal anti-Erv1 rabbit antibody at dilution 1:1000 in 5% milk was applied. For Erv1-RNAi cell line anti-Hsp70 mouse antibody in dilution 1:1000 in 5% milk was used.

Slides were washed 3x 5 min with PBS and then incubated with secondary antibody diluted in 5% milk for 1 hour at RT. For SmOxP9 cells Goat Anti-Rabbit IgG at a dilution 1:1000 was used. For Erv1-RNAi cells Goat Anti-Mouse IgG dissolved at a dilution of 1:1000 was used. Both samples were also prepared without the application of the secondary

antibody to serve as negative controls (data not shown). The slides were washed 5x 5 min with PBS, mounted with 1 drop of mounting media with DAPI under the cover glass and sealed airtight with a transparent nail polish. The slides were stored in the dark at 4°C until use, and were observed under a fluorescent microscope. Image manipulations were performed using ImageJ.

### 3. 4. 2. Selective permeabilization with digitonin

» *Principle:* Since digitonin is a non-ionic detergent, it is able to disrupt cell membranes, so that components located on the inner faces of isolated membrane vesicles, or in the solution within them, are made accessible and can be assayed. Thus depending upon the digitonin concentration, we are able to solubilize distinct subcellular compartments in successive steps, in such a way that the membranes lying further inside of the cell are accessed later (i.e. at higher digitonin concentrations) than the outer membranes. Individual fractions of increasing digitonin concentrations are then analysed using SDS PAGE, employing specific antibodies against marker proteins (antigens previously shown to be localized at known cellular sites), so that we can distinguish the degree of purity for each of the fractions and further define the intracellular location of the protein of interest [115].

Tab. 6: Materials used for selective permeabilization with digitonin.

| | |
|---|---|
| 1x PBS | 137 mM NaCl, 2.7 mM KCl, 4.3 mM $Na_2HPO_4$, 1.47 mM $KH_2PO_4$, pH 7.4 |
| STE-NaCl buffer | 25 mM Tris, pH 7.4, 250 mM sucrose, 1 mM EDTA, 150 mM NaCl |
| Digitonin | 1% digitonin in MiliQ $H_2O$ |
| 5x Sample Buffer | 96 mM Tris-HCl, 40% glycerol, 8% (v/v) β-mercaptoethanol, 0.16% bromophenol blue, pH 6.8 |

» *Procedure:* Cells were grown in SDM-79 medium with appropriate drugs in concentrations between 0.5-1x$10^7$ cells/mL, 2.2x$10^9$ cells were harvested by centrifugation at 1000 g, and 4°C for 10 min and washed once with PBS. The cell pellet was resuspended in STE-NaCl buffer (150 µL/2x$10^8$ cells), and the cell suspension was then split into 150 µL aliquot parts. These aliquots were filled in to a final volume of 300 µL with STE-NaCl buffer and STE-NaCl-buffer enriched with digitonin (see Tab. 7), so that the final digitonin concentrations ranging from 0 to 1.5 mM were obtained. Samples were mixed, incubated for 4 min at RT and spun at 14000 g, at RT for 2 min. 200 µL of the supernatant were collected, mixed with 50 µL 5x Sample buffer, boiled for 5 min and then stored at -20°C until further analysed by Western blot.

Table 7: Preparation of digitonin gradient for subcellular fractination.

| Sample Number | 1 | 2 | 3 | 4 | 5 | 6 | 7 | 8 | 9 | 10 |
|---|---|---|---|---|---|---|---|---|---|---|
| Final digitonin concentration [mM] | 0 | 0.05 | 0.1 | 0.2 | 0.3 | 0.4 | 0.6 | 0.8 | 1.0 | 1.5 |
| Cell suspension [µL] | 150 | 150 | 150 | 150 | 150 | 150 | 150 | 150 | 150 | 150 |
| STE-NaCl buffer [µL] | 150 | 142.5 | 135 | 120 | 105 | 90 | 60 | 30 | 10 | 105 |
| STE-NaCl buffer with 2.0 mM digitonin [µL] | 0 | 7.5 | 15 | 30 | 45 | 60 | 90 | 120 | 140 | 0 |
| STE-NaCl buffer with 10 mM digitonin [µL] | 0 | 0 | 0 | 0 | 0 | 0 | 0 | 0 | 0 | 45 |

### 3. 4. 3. Sodium Dodecyl Sulphate Polyacrylamide Gel Electrophoresis

» *Principle:* Sodium Dodecyl Sulphate Polyacrylamide Gel Electrophoresis (SDS-PAGE) is a biochemical method used to separate proteins according to the differences in their molecular mass. Since proteins consist of polypeptide chains of amino acid residues displaying heterogeneous biochemical properties and hence they tend to form higher-order structures, a chemical and physical denaturant is applied prior to analysis. Proteins are first treated with Sample Buffer containing β-mercaptoethanol, a mild reducing agent that can reduce disulfide bonds, while SDS, which is present both in the gel and the running buffer, can efficiently disrupt hydrophobic and ionic interactions. Additionally the sample is usually boiled which further helps to disrupt the secondary structure of proteins and allows better accessibility by the applied denaturants. Proteins are thus denatured to approximately linear forms and ‘coated’ with a monolayer of negatively charged SDS molecules, as a result the migration rate of proteins is inversely proportional to their molecular sizes.

The gel consists of two layers of different polyacrylamide concentrations and pH values, the (5%) stacking gel serves as a solid matrix, to focus samples into a narrow band, thus providing a clear-cut line of discontinuity. Samples then enter the (15%) running gel where the proteins get separated according to their size. A molecular-weight size marker, a set of standards, is run in a separate lane of the gel, so that the approximate molecular mass of molecules assayed can be determined [115].

Tab. 8: Materials used for SDS-PAGE.

| | |
|---|---|
| Stacking gel | 5% acrylamide, 125mM Tris-HCl, pH 6.8, and 0.1% SDS, 0.1% ammonium persulfate, 0.005% TEMED |
| Running gel | 12% acrylamide, 375 mM Tris-HCl, pH 8.8 and 0.1% SDS, 0.1% ammonium persulfate, 0.025% TEMED |
| Running buffer | 5 mM Tris, 38.4 mM glycine, 0.02% SDS |
| Precisions Plus Protein™ Dual Color Standards | (Bio-Rad) |
| 5x Sample Buffer | 96 mM Tris-HCl, 40% glycerol, 8% (v/v) β-mercaptoethanol, 0.16% bromophenol blue, pH 6.8 |

» *Procedure:* For the digitonin fractionation and for analysis of the co-immunoprecipitation procedure, volume corresponding to $1x10^7$ cells was loaded per well. To check for the expression of Erv1-v5 tagged cell line, $5x10^7$ cells were harvested (at 1000 g, and RT, 10 min), washed once and sequentially resuspended in PBS to the concentration of $1x10^9$ cells/mL, appropriate volume of 5x Sample Buffer was added and the sample was boiled at 98°C for 10 min. Volumes corresponding to $1x10^7$ cells were then loaded per well. Commonly 1.5 mm spacer with 15 well combs were used (25 µL wells). Upon preparation of the gel and loading of the samples, the gel was run at 75 V until the samples reached the running gel and then at 125 V till completion.

### 3. 4. 4. Western Blot Analysis

» *Principle:* Western Blotting is a technique used to detect specific proteins within a cellular lysate. The mixture of proteins is first separated by SDS-PAGE. In order to make the proteins accessible to antibody detection they have to be moved from within the gel onto a stable (PVDF or nitrocellulose) membrane. If this transfer is performed electrophoretically, the method is called electroblotting. The membrane is able to non-specifically bind any proteins, therefore steps to prevent non-specific binding of the antibody have to be taken. This is achieved by blocking the membrane with (3-5%) protein solution prior to the application of antibodies. Upon blocking, the membrane is incubated with the primary and the secondary antibodies respectively. The secondary antibody usually carries a conjugated enzyme, and since several molecules of the secondary antibody can bind to one primary antibody, the signal is thus enhanced. Results are visualized by supplying the conjugated enzyme with its substrate so that a detectable product is formed [115].

Tab. 9: Materials used for Western blot analysis.

| | |
|---|---|
| PVDF membrane | (GE Healthcare) |
| Blotting buffer | 25 mM Tris, 386 mM glycine, 3.7 g/L SDS, 20% ethanol) |
| 5% milk | 5% (w/v) Milk powder dissolved in 1x PBS-Tween |
| 1x PBS-Tween | 1x PBS, 0.05% Tween20 |
| Clarity™ Western ECL | (Bio-Rad) |
| **Antibodies:** | |
| Anti-Enolase | (Paul Michels, University of Edinburgh) |
| Anti-Hsp70 | [116] |
| Anti-v5 | (ThermoFisher Scientific, 37-7500) |
| Anti-Erv1 | [104] |
| Rabbit Anti-Mouse IgG | (Sigma-Aldrich, A9044) |
| Goat Anti-Rabbit IgG | (Sigma-Aldrich, A0545) |

» *Procedure:* Protein samples separated by the SDS-PAGE were transferred onto PVDF membrane by wet electro blotting. The PVDF membrane was activated by submersion in methanol for 5 min, samples were blotted for 1,5 hours at 100 V while submerged in the blotting buffer. After completing blotting, the membrane was blocked with 5% milk for 1 hour at RT, or at 4°C over night. Primary antibodies (Anti-Hsp70, Anti-v5, Anti-Erv1) were applied in 1:1000 dilution in 5% milk, Anti-Enolase was applied in 1:2000 dilution, for 2 hours at RT. The membrane was washed 3x 5 min with PBS-Tween and the secondary antibodies were applied in 1:1000 dilution in 5% milk for 1 hour at RT. After washing the membrane 5x 5 min with PBS-Tween the antigen-antibody complexes were visualized by incubating the membrane for 1 min with ECL in the dark. Pictures were taken by signal accumulation exposure on a ChemiDoc MP (Bio Rad) using the Image Lab™ software. Results are shown in the chapters referring to the methods where Western Blot analysis was used for evaluation of the data obtained.

### 3. 5. Co-Immunoprecipitation

» *Principle:* Co-immunoprecipitation is a technique for detection of protein interactions, whereas a protein of interest is precipitated out of solution (cell lysate) using specific antibody. The protein is isolated under conditions in which any other interacting proteins stay associated, so that all possible components of a complex are isolated together – co-immunoprecipitated [108]. During the process, the antibody against the target protein is immobilized on an insoluble matrix, in our case on the magnetic beads, cellular lysate is then applied to this matrix, so the protein of interest is bound together with its interacting partners, while all the other contents of the cellular lysate pass through. The flow through fractions may be collected to facilitate the process of purification. After washing, high pH buffer is usually applied to release and eluate the target protein complex. Effectiveness of the process is determined by SDS-PAGE [115].

#### 3. 5. 1. Preparation of the anti-Erv1 coated beads

Tab. 10: Materials used for preparation of Erv1 coated Dynabeads.

| | |
|---|---|
| Dynabeads® M-270 Epoxy | (ThermoFisher Scientific, 14302D) |
| Anti-Erv1 Antibody | [100] |
| Sodium phosphate solution | 100 mM Na-phosphate, pH 7.4 |
| Ammonium sulphate solution | 3M $(NH_4)_2SO_4$ |
| Glycine solution | 100 mM glycine, pH 2.5 |
| Tris hydrochloride solution | 100 mM Tris-HCl, pH 8.8 |
| Triethylamine solution | 100 mM triethylamine |
| 1x PBS | 137 mM NaCl, 2.7 mM KCl, 4.3 mM $Na_2HPO_4$, 1.47 mM $KH_2PO_4$, pH 7.4 |

» *Procedure:* All solutions were prepared with MiliQ $H_2O$ and were filtered through a 0.22 µm filter before use. 10mg Dynabeads were washed with 1 mL sodium phosphate solution for 15 min at RT, the supernatant was then discarded and the beads were mixed with 200 µL of the anti-Erv1 antibody and 100 µL ammonium sulphate solution, the mixture was incubated for 48 hours at 30°C under continual rotation. The beads were than washed sequentially with 1 mL each of the following solutions: sodium phosphate (5 min), glycine (30 sec), Tris hydrochloride (5 min), triethylamine (30 sec), 2x PBS (5min), 1x PBS + 0.5% (v/v) TX-100 (5 min) and 1x PBS (5 min), in the order stated. The beads were resuspended in 25 µL 1x PBS and stored at 4°C until used. Additionally 10 mg Dynabeads were prepared without the addition of the antibody to serve as negative control (data not shown).

### 3. 5. 2. The Co-Immunoprecipitation procedure

Tab. 11: Materials used for the co-immunoprecipitation procedure.

| | |
|---|---|
| 1x PBS | 137 mM NaCl, 2.7 mM KCl, 4.3 mM $Na_2HPO_4$, 1.47 mM $KH_2PO_4$, pH 7.4 |
| Lysis buffer | 20 mM HEPES, pH 7.4, 150 mM Na-Citrate, 1 mM $MgCl_2$, 0.1 mM $CaCl_2$, 0.1% TX-100, + cOmplete™, EDTA free protein inhibitor (1 tablet per 10 mL buffer) |

» *Procedure:* Cells were grown in SDM-79 medium with appropriate drugs in concentrations between 0.5-1x$10^7$ cells/mL. 3x$10^9$ cells were harvested by centrifugation at 1000 g, at 4°C for 10 min. The cell pellet was washed once and then resuspended in 500 µL 1x PBS. The solution was transferred to a microcentrifuge tube and spun at 1800 g for 3 min, 400 µL of the supernatant were discarded, the pellet was resuspended in the remaining volume of 1x PBS and then mixed with 2 mL lysis buffer. The mixture was incubated for 5 min on ice and then spun at 20 000 g, and 8°C for 20 min. The supernatant was collected and loaded on 25 µL of the bead suspension, the mixture was incubated for 2 hours at 4°C under continuous agitation. The beads were collected and washed 5x 5 min with 1 mL lysis buffer (without Triton X-100), 11 µL of the beads were used for analysis by western blot and silver staining, the remaining amount was stored at -80°C and sent for analysis by Mass Spectrometry to Prague (Service Laboratories of the Biology Section: Laboratory of Mass Spectrometry, Charles University in Prague). The procedure was carried out the same way using the Dynabeads without the bound antibody to serve as negative control.

### 3. 5. 3. Gel Silver Staining

*» Principle:* Silver staining is one of the most sensitive methods of protein detection following SDS-PAGE, consequently it is the method of choice when very low amounts of proteins have to be detected. The technique takes advantage of the ability of proteins to bind silver ions. Under appropriate (reducing) conditions (e. g. formalin fixation), the silver solution is reduced to metallic silver, so that a visible image is created. Fixation with aldehydes dramatically improves fixation, sensitivity and uniformity of the staining, but precludes any other downstream processing.

Many variants of silver staining protocols are available and have to be chosen according to individual needs. Since we did not intend to use the stained gel for mass spectrometry analysis, there was no need to avoid the fixation step using aldehydes. Upon fixation, the general procedure include sensitization and washing to increase the sensitivity and contrast of the staining, impregnation with silver nitrate solution and development to build up the silver metal image. Finally the reaction has to be stopped to prevent excessive background [117].

Tab. 12: Materials used for silver staining of SDS-PAGE gel.

| | |
|---|---|
| Fixer | 40% ethanol, 10% acetic acid, 50% $H_2O$ |
| Sensitizer | 0.02% $Na_2S_2O_3$ |
| Silver nitrate solution | 0.1% $AgNO_3$, 0.02% formaldehyde (added before use) |
| Developer | 3% $Na_2CO_3$, 0.05% formaldehyde (added before use) |
| Terminator | 5% acetic acid |
| MiliQ $H_2O$ | |

*» Procedure:* Upon completion of the SDS-PAGE, the gel was incubated in fixer for 1 hour and washed over night with MiliQ $H_2O$ (with several changes of the water), to get rid of all the traces of acetic acid. Sensitizer was applied for 1 min, and the gel was then washed 3x 20 sec with MiliQ $H_2O$. Afterwards the gel was incubated in cold silver nitrate solution for 20 min, then washed 2x 20 sec and additionally 1 min in a new staining tray. Developer was applied and staining was terminated when the protein bands were sufficiently visible.

### 3. 5. 4. Mass Spectrometry

» *Principle:* Protein mass spectrometry is an analytical technique used for identification and quantification of compounds of a protein complex or for determination of an unknown polypeptide sequence and has also application for structural determination of proteins. First the sample is ionized to generate charged molecules (or fragments of molecules), which are then targeted to the mass analyser, where an electric (or magnetic) field is applied. The magnitude of deflection of the incoming ions trajectory depends on its mass to charge ratio, the lighter ions the bigger magnitude of deflection (according to Newton's law), thus the differences in the masses of the fragments allow the analyser to sort them by their mass to charge ratio. When sorted, the individual fractions of fragments are analysed by a detector, which measures the quantity of an individual fraction and thus provides the abundance of each ion present. Mass spectrum is an ion signal as a function of its mass to charge ratio and is used to elucidate the chemical structure of peptides or other chemical compounds present within the sample. Sequence data are determined by tandem mass spectrometry analysis in the process termed *de novo* peptide sequencing [108].

### 4. 1. v5 tagging

To check for the success of the long primer PCR reaction, the product was analysed by agarose gel electrophoresis. When the gel was examined under UV light, a band of the expected size (~2000 kb) was observed (see Fig. 8 A.). The remaining volume of the PCR product was then used for the electroparation without any additional purification steps. Upon recovery of the cells from the electroporation, positive clones were sorted out using hygromycin as a selection marker. Afterwards we verified the expression of the tagged protein by Western Blot analysis using anti-v5 antibody (see Fig. 8 B.). The size of the expressed protein was in accordance with the size predicted (36, 9 kDa).

From the parental SmOx P9 cell line, a cell line expressing C-terminally endogenously tagged form of Erv1 was successfully generated.

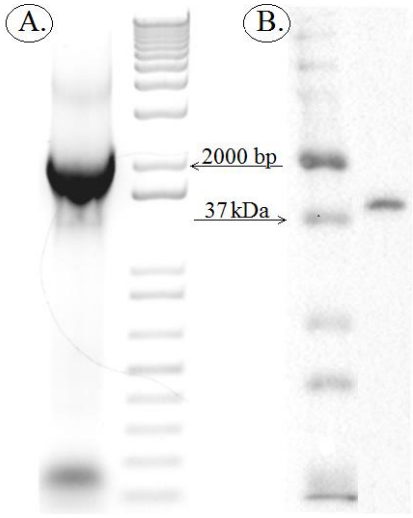


Fig 8.: A. Agarose gel electrophoresis of the PCR product used for the generation of Erv1-v5 tagged cell line. B. Western Blot showing the expression of the Erv1-v5 tagged cell line.

### 4. 2. Erv1-RNAi cell line

#### 4. 2. 1. Growth curve

The Erv1-RNAi cell line was previously constructed by Somsuvro Basu [100]. Upon the RNAi induction, cell densities were measured once per 24 hours, for the duration of ten days in total. The values of the growth rate were counted for wild type, non-induced and induced cells and were compared to each other (Fig. 9). The resulting graph depicts a significant effect of Erv1 silencing on the growth rate, implying that the protein is essential for cell survival. The cell line still showed the growth phenotype as described previously [100] and thus was used for further experiments.

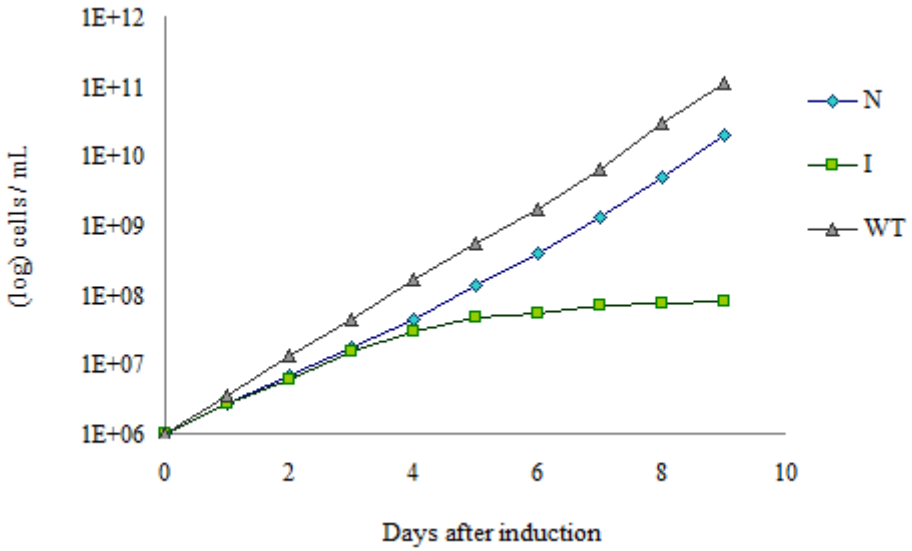


Fig. 9: Growth curve of Erv1-RNAi cell line. The RNAi was induced by addition of tetracycline to the culture medium. Abbreviations: WT – wild type, N – non-induced, I – induced cells.

### 4. 2. 2. Aconitase Activity Measurement

Cytosolic and mitochondrial cellular fractions were prepared to test the effect of Erv1 knock-down on the activity of the iron-sulphur cluster enzyme, aconitase, thereby examining the effect of the depletion of Erv1 on both the mitochondrial (ISC) and the cytosolic (CIA) [Fe-S] machineries. Purity of the prepared fractions was verified by Western Blot analysis using antibodies against known marker proteins (data not shown).

Aconitase activity was determined, by the concentration of product formed by the enzyme within 10 min, per total protein amount. Values of the aconitase activity counted for the induced cells were compared relative to that of non-induced cells (see Fig. 10). A significant decrease in the aconitase activity was observed in both mitochondrial and cytosolic fractions, in particular the activity in mitochondria was reduced to ~30%, while the activity in cytosol dropped as much as to ~10%. The results thus indicate that along with the gradual protein depletion, both ISC and CIA machineries are subsequently impaired.

### 4. 2. 3. Mitochondrial Membrane Potential Measurement

In order to further examine the possible abnormalities following the knock-down of Erv1, we utilized the method for the quantitative measurement of the mitochondrial membrane potential *in situ*. The measurement revealed that down-regulation of Erv1 cause significant decrease in the mitochondrial membrane potential (see Fig. 11), whereas on the fourth day of induction it is reduced to ~50%. The results indicate that the role of Erv1 is important for the maintenance of functional mitochondria, and thus Erv1 is most probably involved in the mitochondrial protein import.

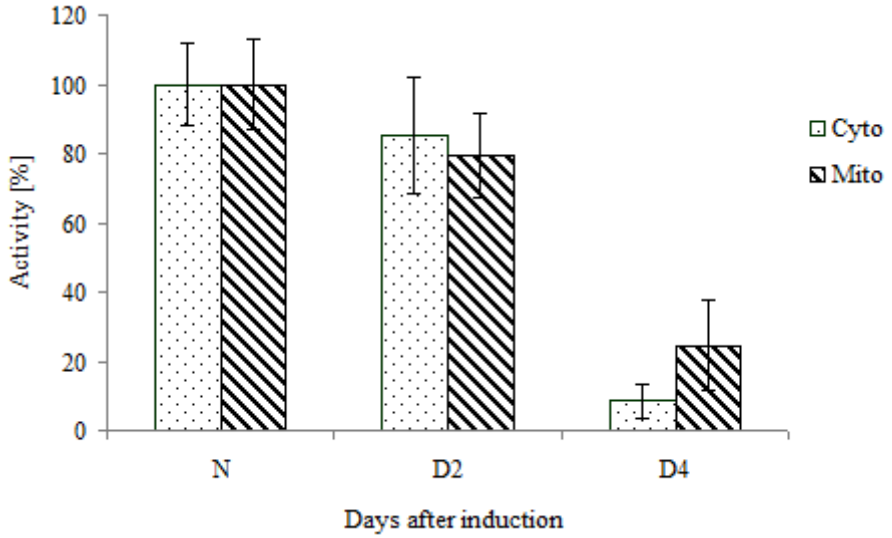


Fig. 10: Aconitase activity for Erv1 knock-down, shown as induced relative to non-induced. Error bars show 95% confidence interval.

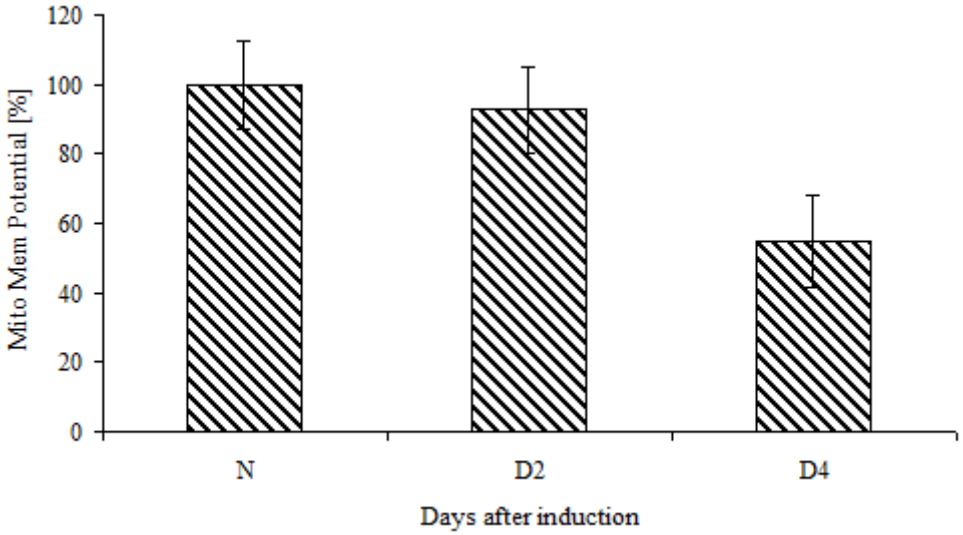


Fig. 11: Analysis of decrease in mitochondrial membrane potential during apoptosis using MitoTracker® Red dye. Abbreviations: N – non-induced. Error bars show 95% confidence interval.

### 4. 2. 4. Aberrant Mitochondrial Morphology determined by IFA

Immunofluorescence assay was utilized to visualize possible changes of the mitochondrial morphology following the RNAi induction. For staining of the mitochondria we used the mitochondrial matrix marker protein mtHsp70, as MitoTracker Red could not properly enter the organelle due to the decreased membrane potential. For staining of the DNA mounting media with DAPI was used.

Following the induction of the RNAi cell line remarkable changes in the mitochondrial morphology were observed. Even though the RNAi expression system was previously reported to be leaky (Erv1 is down-regulated already in non-induced cells) [100], this “imperfection” was not evident with regard to the mitochondrial morphology, as the

non-induced cells show approximately the same mitochondrial pattern as the parental wild type cell line (see Fig. 12). Upon the induction of the RNAi, gradual collapse of the mitochondrial network follows; aberrant mitochondrial morphology was evident already on the second day of induction, when the mitochondria tend to loose branching, starting from the anterior and the posterior end of the cell, still leaving a branched section in the middle of the cell, surrounding the nucleus (Fig. 12). On the fourth day of induction the mitochondria was observed as a single line, upon prolonged induction, the cells show elongated morphology and finally their mitochondria gets fragmented, which progressively leads to cell death.

The results again show that Erv1 is important for the maintenance of functional mitochondria, giving the evidence for its involvement in the mitochondrial protein import.

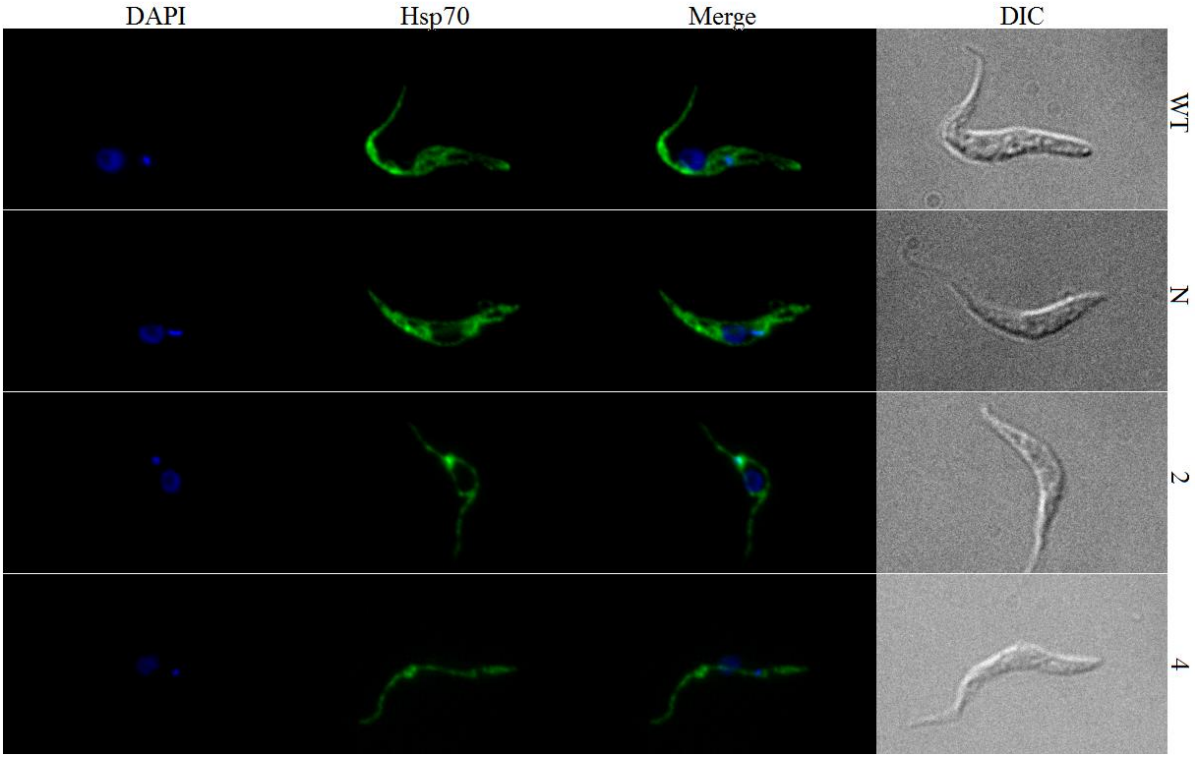


Fig. 12: Aberrant mitochondrial morphology observed upon the RNAi induction. DAPI/blue/DNA, Hsp70/green/mitochondria. Abbreviations: WT – wild type, N – non-induced, 2, 4 – days of RNAi induction.

### 4. 3. Localization

#### 4. 3. 1. Localization by IFA

Immunofluorescence assay was used for the localization of TbErv1 using polyclonal anti-Erv1 antibody. For staining we used: mounting media with DAPI for DNA, secondary antibodies with conjugated fluorophore for the protein of interest, MitoTracker Red for mitochondria.

Our protein of interest was shown to co-localize well with the mitochondrial marker (see Fig. 13), suggesting for mitochondrial localization of TbErv1. To differentiate between

the mitochondrial subcompartments a detailed study using selective permeabilization with digitonin was performed (see Fig. 14).

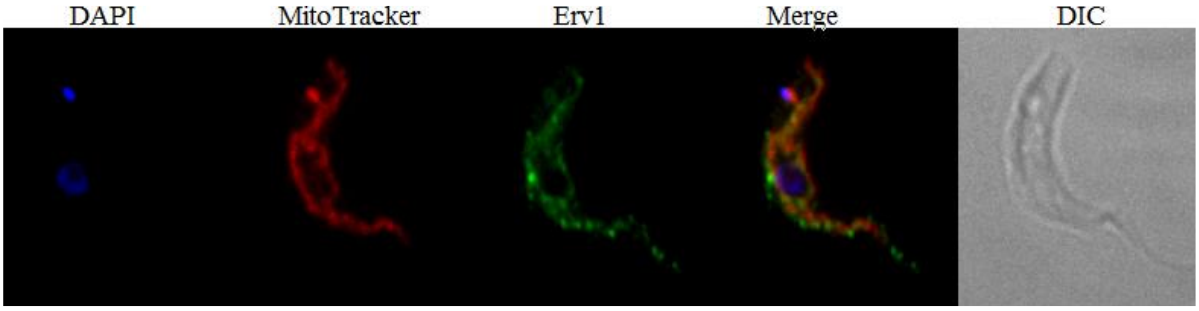


Fig. 13: IFA of representative cell for Erv1 localization. DAPI/blue/DNA, MitoTracker/red/mitochondria, anti-Erv1 Ab/green/Erv1.

### 4. 3. 2. Localization by Selective Permeabilization with Digitonin

In order to distinguish the exact localization of Erv1 within the four mitochondrial subcompartments, selective permeabilization with digitonin was utilized. Cells were exposed to digitonin concentrations ranging from 0,05 to 1,5 mM, and the lysates obtained were then analysed by Western Blot using antibodies against Erv1, and against the known marker proteins; enolase as cytosolic marker, and mtHsp70 as mitochondrial matrix marker. The assay shows that the v5 tagged version of Erv1 (Erv1-v5) is released in fractions of lower digitonin concentration, in comparison to the natural form of Erv1 (see Fig. 14), suggesting the tag is interfering with the protein localization. Thereby the Erv1-v5 tagged cell line was decided not to be used for further experiments.

Regarding TbErv1 localization, the protein was released in a fraction of higher digitonin concentration in comparison to cytosolic marker, and at the same time in a fraction of lower digitonin concentration than mitochondrial matrix marker. The results suggest Erv1 is localized either to the outer mitochondrial membrane or to the intermembrane space.

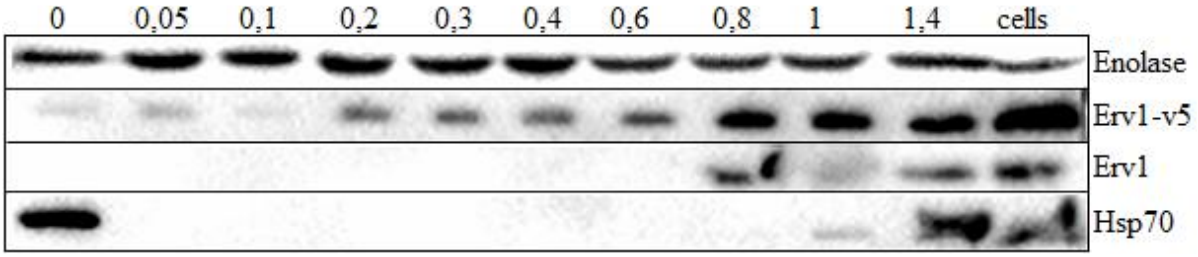


Fig.14: Selective permeabilization with digitonin for the Erv1-v5 tagged cell line using anti-v5 and anti- Erv1 antibody. Numeral labeling represents the digitonin concentrations [mM] applied in the respective fractions.

### 4. 5. Co-Immunoprecipitation

While majority of the sample was sent for analysis by Mass Spectrometry, a smaller fraction was analysed using Western Blot and Gel Silver Staining. The results show that protein of the size expected (30 kDa) was pulled down (see Fig. 15), while it was not present in the negative control. The first samples represent the release of Erv1 into the solution, following the addition of the lysis buffer, a degradation product or possibly an isoform of Erv1 was additionally detected in the lysate. The excessive bands observed in the sample of the beads are indeed coming from the antibody light (~20 kDa) and heavy (~50 kDa) chains.

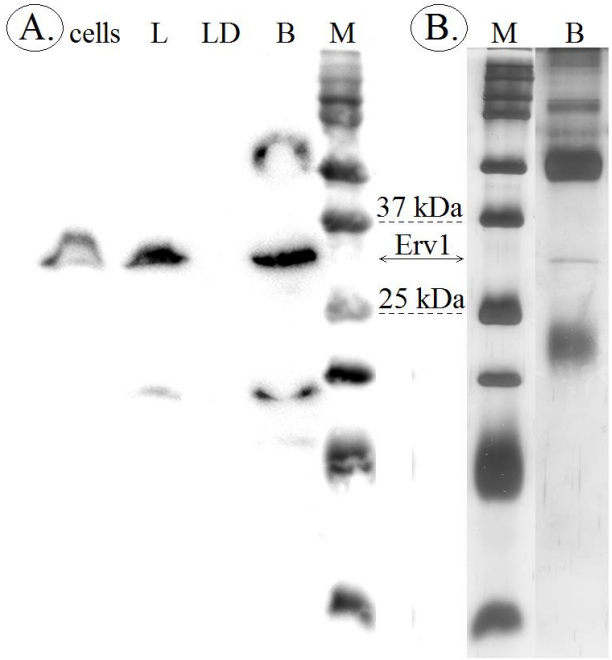


Fig. 15: A. Western Blot analysis, B. Silver Staining.
Abbreviations: cells, L/lysate, LD/loading dye, B/beads, M/marker.

### 4. 6. Mass Spectrometry

From the Mass Spectrometry we obtained results showing sequences of proteins found within the sample, their abundances, and fold change of the abundances over the control sample. The sequences were analysed over an identification pipeline against the Uniprot database. The identified proteins were lined up according to their relative abundances, the top seven most abundant proteins in comparison to the control sample are listed below (see Tab. 13).The results show that the target protein was detected as the most abundant one, additionally other mitochondrial proteins including mitochondrial membrane-bound proteins and membrane proteins of other organelles were co-purified.

Tab. 13: Results obtained from the Mass Spectrometry. Abbreviation: mt - mitochondrial.

| Name | TriTryp Accession | Relative Abundance | Fold change over control | Localization |
|---|---|---|---|---|
| Sulfhydryl oxidase, Erv1 | Tb927.9.6060 | 1.111E+09 | 57.02687 | Mt outer membrane |
| Tryparedoxin peroxidase | Tb09.160.4250 | 1.134E+07 | 1.703925 | Cytosol |
| Mitochondrial carrier protein, putative | Tb927.10.14840 | 7.585E+06 | 3.325866 | Mt inner memrane |
| Gim5B protein | Tb09.211.2740 | 7.429E+06 | 2.387482 | Peroxisomal mem |
| Cytochrome C oxidase subunit IV | Tb927.1.4100 | 6.513E+06 | 6.589870 | Mt inner membrane |
| Glyceraldehyde-3-phosphate dehydrogenase | Tb927.6.4300 | 6.437E+06 | 1.378751 | Glycosome |
| Protein Associated with Differentiation (PAD1, PAD2) | Tb927.7.5940, Tb927.7.5930 | 4.258E+06 | 3.138619 | Plasma membrane |

### 5. 1. PCR only tagging

A cell line expressing the tagged protein was successfully generated, follow-up experiments however revealed that the C terminal tag has significant influence on the subcellular localization of the protein and thus may also interfere with the protein function.

Results suggest that the C terminal (KISS) domain [101] may either contain a targeting sequence (which cannot be predicted) or possibly the domain is important for proper folding of the protein. The anomalous targeting therefore may only be a consequence of aberrant folding resulting from an interaction between the KISS domain and the newly introduced C terminal tag. As the technique was previously utilized by other members of our laboratory and showed no effect on mitochondrial targeting (unpublished data), we suppose the misslocalization of Erv1 due to the tagging is protein specific.

### 5. 2. RNAi cell line

#### 5. 2. 1. Growth curve

The growth curve recorded showed that the previously constructed RNAi cell line [100] was still intact and therefore suitable for utilization in other experiments. The results imply that Erv1 is an essential protein, as it was already shown previously [100].

#### 5. 2. 2. Aconitase Activity Measurement

The aconitase activity measurement showed that the knock-down of Erv1 had a significant influence on both mitochondrial and cytosolic iron sulphur cluster assembly machineries.

For the knock-down of members of the ISC-export machinery, only defects in the CIA machinery were reported [24, 59]. The defects in CIA are assumed to be caused by lack of the unknown sulphur containing compound required for the formation of [Fe-S]s in cytosol, since the compound cannot be exported out of mitochondria, where it is produced by the ISC machinery [54].

An influence only on the CIA machinery was previously reported also for the knock-down of ScErv1, and therefore Erv1 was proposed to take a part in the ISC-export machinery [87]. The idea was further supported by the observations of changes in mitochondrial morphology and distribution as well as loss of mitochondrial genome, following ScErv1 knock-down [86], as such phenotype was previously also described for the knock-down of ScAtm1 [118]. Hence the cooperation of these two proteins in the export of the unknown

compound was suggested [54]. The decrease of the aconitase activity in cytosol could therefore be the result of an impairment of the ISC export machinery, assuming that Erv1 is an essential component of this pathway, which however does not provide an explanation for the decrease in the mitochondrial aconitase activity. Furthermore, a recent study suggests that cytosolic [Fe-S] maturation is independent of Erv1 [120].

Erv1 however also plays a role in the import of cysteine-rich proteins into the IMS of mitochondria, or in the MIA pathway to be exact [69]. The substrates of the MIA pathway include e. g. small Tim chaperones [67], which are required for the assembly of larger complexes, which negotiate protein transport across the mitochondrial inner membrane [72]. Thus upon Erv1 depletion, the mitochondrial protein import to the IMS [66, 69] and consequently the import to the mitochondrial matrix are gradually inhibited. Since cysteine-rich proteins serve as the source of sulphur for the ISC machinery [40], the decreased mitochondrial aconitase activity may be a consequence of defective mitochondrial protein import and is resulting in lack of substrates for the cysteine desulphurase to generate the sulphur atom required for the formation of [Fe-S]s inside mitochondria. Therefore the previously reported decrease in the activity of cytosolic [Fe-S] protein [87], is not necessarily a consequence of the impairment of the ISC export machinery, and thus may be considered to be a secondary phenotype to the knock-down of Erv1.

### 5. 2. 3. Aberrant Mitochondrial Morphology determined by IFA

The IFA was utilized for tracing the changes of mitochondrial morphology following the knock-down of Erv1, as already reported previously in yeast and *T. brucei* [86, 100]. The aberrant mitochondrial morphology was evident already on the second day of RNAi induction, when the cells displayed morphological changes strikingly resembling gradual collapse of the mitochondrial network. Upon prolonged induction the mitochondria was subjected to fragmentation, which consequently led to the loss of viability of the cells. The observed phenotype was additionally accompanied by decreased mitochondrial membrane potential. It was reported that depletion of Erv1 in yeast prevents the import of IMS precursors, and is therefore lethal for the cells [66, 70]. Since the aberrant mitochondrial morphology is a common feature to defective mitochondrial protein import pathways [119], we can affirm the participation of TbErv1 in this process. Thus we suggest TbErv1 presumably functions in the mitochondrial protein import despite the natural absence of a Mia40 homologue. The exact mechanism of the import reaction however stays for debate, since such function of Erv1 was still not shown in any eukaryote lacking a Mia40 homologue.

### 5. 3. Localization

The localization of Erv1 by IFA showed mitochondrial pattern, as it was already reported previously in yeast [87]. The selective permeabilization with digitonin further revealed that Erv1 is released in a fraction of higher digitonin concentration compared to cytosolic marker, and at the same time it is released in a fraction of lower digitonin concentration compared to mitochondrial matrix marker. The results thus indicate Erv1 is either located to the outer mitochondrial membrane or into the IMS. To be able to differentiate between the two possibilities, antibodies against known marker proteins of the outer mitochondrial membrane are required, yet were not available in our laboratory. Antibodies against ATOM and VDAC were tested, the first protein was however found to be too large to be detected by Western Blot and the second is linked to the inner membrane, which is probably the reason why it was observed to be released in the same fraction as the mitochondrial matrix marker. Since the permeabilization and solubilization of the outer mitochondrial membrane automatically leads to the release of the IMS, the utilized method is not suitable to resolve this issue. Samples were therefore sent for analysis by electron microscopy to find the final answer on the localization of Erv1 in Trypanosomes, the results are currently not yet available.

### 5. 4. Co-Immunoprecipitation & Mass Spectrometry

Even though the cells were not mechanically disrupted, our results show that the conditions chosen are in principle suitable for the detection of IMS-localized as well as membrane-bound proteins, as proteins of various membranes and mitochondrial compartments were released and identified by means of the mass spectrometry.

With respect to the mass spectrometry results, the role of TbErv1 in the ISC-export machinery is in dispute, as TbAtm1 was not under the proteins enriched. These findings however do not contradict the claim that TbErv1 still can take a part in the biogenesis of [Fe-S] proteins. The exact site of action however could not be determined.

None of the proteins which were co-purified together with TbErv1 seems to be capable of performing a function similar to that of ScMia40 in yeast. First, none of the identified proteins is localized to the IMS of mitochondria. And second, none of the proteins display ScMia40 motif neither possess a CPC motif, which is fundamental for ScMia40 function [79]. Therefore we suggest TbErv1 can function in mitochondrial protein import despite the natural absence of a Mia40 homologue, which is further supported by the observation of aberrant mitochondrial morphology following the knock-down of TbErv1

[119], which was additionally accompanied by the decreased mitochondrial membrane potential.

In summary we propose TbErv1 alone is able to perform its role in the mitochondrial import and/or export. Our findings are in accordance with the previously published study suggesting that the different arrangement of cysteine pairs in TbErv1 may allow Erv1 alone to function as a replacement of the MIA pathway [102].

Still the interaction between TbErv1 and its potential interaction partners may be very transient and therefore could not be detected using this procedure.

# 6. CONCLUSIONS

We found TbErv1 is localized either to the outer membrane or to the intermembrane space of mitochondria. This issue will be resolved by the electron microscopy.

The exact site of action of TbErv1 in the iron-sulphur cluster protein biogenesis was not determined. We suppose TbErv1 is not likely to be involved in the ISC-export machinery, as Atm1 was not identified by mass spectrometry. The results from the aconitase activity measurement may suggest for the involvement of TbErv1 in the ISC machinery. We however hypothesize that the ISC machinery is impaired as a consequence of the defective mitochondrial protein import.

We suggest that TbErv1 may function in the import of cysteine-rich proteins into mitochondria despite the natural absence of a Mia40 homologue.

No interaction partner, which possibly could assist in one of the processes where Erv1 was proposed to take a part, was identified.

# 7. LITERATURE CITED


[1] Verner Z, Paris Z, Lukeš J: Mitochondrial membrane potential-based genome-wide RNAi screen of *Trypansoma brucei*. Parasitology Research (2010) 106:1241–1244.

[2] Human African trypanosomiasis. World Health Organization. Available: http://www.who.int/trypanosomiasis_african/parasite/en/. Last accessed 20th March 2016.

[3] Serricchio M, Bütikofer P: *Trypanosoma brucei*: a model micro-organism to study eukaryotic phospholipid biosynthesis. FEBS Journal (2011) 278:1035–1046.

[4] Qingliang L, Luhua L: Prediction of potential drug targets based on simple sequence properties. BMC Bioinformatics (2007) 8:353.

[5] Berriman M, Ghedin E, Hertz-Fowler C, Blandin G,Renauld H, Bartholomeu DC, Lennard NJ, Caler E, Hamlin NE, Haas B et al.: The genome of the African trypanosome *Trypanosoma brucei*. Science (2005) 309(5733): 416–422.

[6] Ngo H, Tschudi C, Gull K, Ullu E: Double-stranded RNA induces mRNA degradation in *Trypanosoma brucei*. Proceedings of the National Academy of Sciences of the USA (1998) 95(24):14687–14692.

[7] Gupta S, Schoer RA, Egan JE, Hannon JG, Mittal V: Inducible, reversible, and stable RNA interference in mammalian cells. Proceedings of the National Academy of Sciences of the USA (2004) 101(7):1927-1932.

[8] Blum B, Bakalara N, Simpson L: A model for RNA editing in kinetoplastid mitochondria: "guide" RNA molecules transcribed from maxicircle DNA provide the edited information. Cell (1990) 60(2):189–198.

[9] Sutton RE, Boothroyd JC: Evidence for trans splicing in trypanosomes. Cell (1986) 47(4):527–535.

[10] Fenn K, Matthews KR: The cell biology of *Trypanosoma brucei* differentiation. Current Opinion in Microbiology (2007) 10(6):539–546.

[11] Langousis G, Hill KL: Motility and more: the flagellum of *Trypanosoma brucei*. Nature Reviews Microbiology (2014) 12(7):505-518.

[12] Lill R, Dutkiewicz R, Elsässer HK, Hausmann A, Netz DJA, Pierik AJ, Stehling O, Urzica E, Mühlenhoff U: Mechanisms of iron–sulphur protein maturation in mitochondria, cytosol and nucleus of eukaryotes. Biochimica et Biophysica Acta (2006) 1763(7):652–667.

[13] Lill R, Mühlenhoff U: Iron–sulphur-protein biogenesis in eukaryotes. TRENDS in Biochemical Sciences (2005) 30(3):133-140.

[14] Lill R, Srinivasan V, Mühlenhoff U: The role of mitochondria in cytosolic-nuclear iron–sulphur protein biogenesis and in cellular iron regulation. Current Opinion in Microbiology (2014) 22:111–119.

[15] Sheftel A, Stehling O, Lill R: Iron–sulphur proteins in health and disease. Trends in Endocrinology and Metabolism (2010) 21(5):302-14.

[16] Frazzon J, Dean DR: Formation of iron-sulphur clusters in bacteria: an emerging field in bioinorganic chemistry. Current Opinion in Chemical Biology (2003) 7:166–173.

[17] Beinert H, Hol RH, Münck E: Iron-sulphur clusters: nature's modular, multipurpose structures. Science (1997) 277:653-659.

[18] Lill R, Mühlenhoff U: Maturation of iron-sulphur proteins in eukaryotes: mechanisms, connected processes, and diseases. Annual Review of Biochemistry (2008) 77:669–700.

[19] Takahashi Y, Tokumoto U: A third bacterial system for the assembly of iron–sulphur clusters with homologs in archaea and plastids. Journal of Biological Chemistry (2002) 277(32):28380–3.

[20] Ali V et al. (2004): An intestinal parasitic protist, *Entamoeba histolytica*, possesses a non-redundant nitrogen fixation-like system for iron–sulphur cluster assembly under anaerobic conditions Journal of Biological Chemistry (2004) 279(16):16863–16874.

[21] Johnson DC, Dean DR, Smith AD, Johnson MK: Structure, function and formation of biological iron–sulphur clusters. Annual Review of Biochemistry (2005) 74:247–281.

[22] Balk J, Lill R: The cell's cookbook for iron–sulphur clusters: recipes for fool's gold?. ChemBioChem (2004) 5:1044–1049.

[23] Lill R, Kispal G: Maturation of cellular Fe/S proteins: the essential function of mitochondria. Trends in Biochemical Sciences (2000) 25(8): 352–356.

[24] Kispal G, Csere P, Prohl C, Lill R: The mitochondrial proteins Atm1p and Nfs1p are required for biogenesis of cytosolic Fe/S proteins. EMBO Journal (1999) 18(14):3981–3989.

[25] Lange H, Kispal G, Kaut A, Lill R: A mitochondrial ferredoxin is essential for biogenesis of intra- and extra-mitochondrial Fe/S proteins. Proceedings of the National Academy of Sciences of the USA (2000) 97:1050-1055.

[26] Stehling O, Lill R: The Role of Mitochondria in Cellular Iron–Sulphur Protein Biogenesis: Mechanisms, Connected Processes, and Diseases. Cold Spring Harbor Perspectives in Biology (2013) 5(8): a011312.

[27] Yuvaniyama P, Agar JN, Cash VL, Johnson MK, Dean DR: NifS-directed assembly of a transient [2Fe–2S] cluster within the NifU protein. Proceedings of the National Academy of Sciences of the USA (2000) 97:599–604.

[28] Dolezal P, Smíd O, Rada P, Zubácová Z, Brusać D, Suták R, Nebesárová J, Lithgow T, Tachezy J: Giardia mitosomes and trichomonad hydrogenosomes share a common mode of protein targeting. Proceedings of the National Academy of Sciences of the USA (2005) 102(31):10924–10929.

[29] Hjort K, Goldberg VA, Tsaousis DA, Hirt PR, Emblez MT: Diversity and reductive evolution of mitochondria among microbial eukaryotes. Philosophical Transations of the Royal Society of London. Series B, Biological Sciences (2010) 365(1541):713–727.

[30] van der Giezen M, Tovar J (2005): Degenerate mitochondria. EMBO Reports (2005) 6(6):525–530.

[31] Sutak R, Dolezal P, Fiumera HL, Hrdy I, Dancis A, Delgadillo-Correa M, Johnson PJ, Muller M, Tachezy J: Mitochondrial-type assembly of FeS centers in the hydrogenosomes of the amitochondriate eukaryote *Trichomonas vaginalis*. Proceedings of the National Academy of Sciences of the USA (2004) 101(28):10368–10373.

[32] Klinge S, Hirst J, Maman JD, Krude T, Pellegrini L: An iron–sulphur domain of the eukaryotic primase is essential for RNA primer synthesis. Nature Structural & Molecular Biology 14(9): 875–877.

[33] Rudolf J, Makrantoni V, Ingledew WJ, Stark MJ, White MF: The DNA repair helicases XPD and FancJ have essential iron–sulphur domains. Molecular Cell (2006) 23(6): 801–808.

[34] Kispal G, Sipos K, Lange H, Fekete Z, Bedekovics T, Janaky T, Bassler J, Aguilar Netz DJ, Balk J, Rotte C, et al.: Biogenesis of cytosolic ribosomes requires the essential iron–sulphur protein Rli1p and mitochondria. EMBO Journal (2005) 24(3): 589–598.

[35] Dong J, Lai R, Nielsen K, Fekete CA, Qiu H, Hinnebusch AG: The essential ATP-binding casette protein RLI1 functions in translation by promoting preinitiation complex assembly. Journal of Biological Chemistry (2004) 279(40): 42157-68.

[36] Uringa JE, Zouds JL, Lisaingo K, Lansdorp MP, Boulton JS: RTEL1: an essential helicase for telomere maintenance and the regulation of homologous recombination. Nucleic Acids Research (2011) 39(5):1647–1655.

[37] Lill R, Fekete Z, Sipos K, Rotte C: Is there an answer? Why are mitochondrial essential for life?. IUBMB Life (2005) 57(10): 701 - 703.

[38] Garland AS, Hoff K, Vickerz EL, Culotta CV: *Saccharomyces cerevisiae* ISU1 and ISU2: members of a well-conserved gene family for iron-sulphur cluster assembly. Journal of Molecular Biology (1999) 294(4):897-907.

[39] Lill R: Function and biogenesis of iron-sulphur proteins. Nature (2009) 460:831–838.

[40] Mühlenhoff U, Balk J, Richhardt N, Kaiser TJ, Sipos K, Kispal G, Lill R: Functional characterization of the eukaryotic cysteine desulphurase Nfs1p from *Saccharomyces cerevisiae*. The Journal of Biological Chemistry (2004) 279(35):36906 –36915.

[41] Agar JN, Krebs C, Frayyon J, Huznh BH, Dean DR, Johnson MK: IscU as a scaffold for iron-sulphur cluster biosynthesis: sequential assembly of [2Fe-2S] and [4Fe-4S] clusters in IscU. Biochemistry (2000) 39(27):7856–7862.

[42] Adam CA, Bornhövd C, Prokisch H, Neupert W, Hell K: The Nfs1 interacting protein Isd11 has an essential role in Fe/S cluster biogenesis in mitochondria. EMBO Journal (2006) 25(1): 174–183.

[43] Mühlenhoff U, et al.: Characterization of iron–sulphur protein assembly in isolated mitochondria: a requirement for ATP, NADH and reduced iron. Journal of Biological Chemistry (2002) 277(33):29810–29816.

[44] Foury F, Roganti T: Deletion of the mitochondrial carrier genes MRS3 and MRS4 suppresses mitochondrial iron accumulation in a yeast frataxin-deficient strain. Journal of Biological Chemistry (2002) 277(27):24475-24483.

[45] Li H, Gakh O, Smith DY 4th, Isaya G: Oligomeric yeast frataxin drives assembly of core machinery for mitochondrial iron-sulphur cluster synthesis. Journal of Biological Chemistry (2009) 284(33): 21971-21980.

[46] Webert H, Freibert AS, Gallo A, Heidenreich T, Linne U, Amlacher S, Hurt E, Mülenhoff U, Banci L, Lill R: Functional reconstitution of mitochondrial Fe/S cluster synthesis on Isu1 reveals the involvement of ferredoxin. Nature Communications (2014) 5:5013.

[47] Li J, Saxena S, Pain D, Dancis A: Adrenodoxin reductase homolog (Arh1p) of yeast mitochondria required for iron homeostasis. Journal of Biological Chemistry (2001) 276(2):1503–1509.

[48] Uzarska AM, Dutkiewicz R, Freibert AS, Lill R, Mühlenhoff U: The mitochondrial Hsp70 chaperone Ssq1 facilitates Fe/S cluster transfer from Isu1 to Grx5 by complex formation. Molecular Biology of the Cell (2013) 24(12):1830–1841.

[49] Dutkiewicz R, Schilke B, Kneiszner H, Walter W, Craig EA, Marszalek J: Ssq1, a mitochondrial Hsp70 involved in iron-sulphur (Fe/S) center biogenesis: Similarities to and differences from its bacterial counterpart. Journal of Biological Chemistry (2003) 278(32):29719–29727.

[50] Dutkiewicz R, Schilke B, Cheng S, Knieszner H, Craig EA, Marszalek J: Sequence-specific interaction between mitochondrial Fe–S scaffold protein Isu and Hsp70 Ssq1 is essential for their in vivo function. Journal of Biological Chemistry (2004) 279(28):29167–29174.

[51] Lutz T, Westermann B, Neupert W, Herrmann JM: The mitochondrial proteins Ssq1 and Jac1 are required for the assembly of iron sulphur clusters in mitochondria. Journal of Molecular Biology (2001) 307(3):815-825.

[52] Mühlenhoff U, Gerber J, Richhardt N, Lill R: Components involved in assembly and dislocation of iron-sulphur clusters on the scaffold protein Isu1p. EMBO Journal (2003) 22(18):4815–4825.

[53] Paul DV, Lill R: SnapShot: Eukaryotic Fe-S Protein Biogenesis. Cell Metabolism (2014) 20(2):384-385.

[54] Lill R. et al.: The essential role of mitochondria in the biogenesis of cellular iron-sulphur proteins. Biological Chemistry (1999) 380(10):1157-1166.

[55] Kohlhaw GB: Leucine biosynthesis in fungi: entering metabolism through the back door. Microbiology and Molecular Biology Reviews (2003) 67(1):1-15.

[56] Kuhnke G, Neumann K, Mühlenhoff U, Lill R: Stimulation of the ATPase activity of the yeast mitochondrial ABC transporter Atm1p by thiol compounds. Molecular Membrane Biology (2006) 23(2):173-184.

[57] Srinivasan V, Pierik AJ, Lill R: Crystal structures of nucleotide-free and glutathione-bound mitochondrial ABC transporter Atm1. Science (2014) 343(6175):1137-1140.

[58] Bihlmaier K, Mesecke N, Teryizska N, Bien M, Hell K, Herrmann MJ: The disulfide relay system of mitochondria is connected to the respiratory chain. The Journal of Cell Biology (2007) 179(3):389–395.

[59] Sipos K, Lange H, Fekete Z, Ullmann P, Lill R, Kispal G: Maturation of cytosolic iron–sulphur proteins requires glutathione. Journal of Biological Chemistry (2002) 277(30): 26944-26949.

[60] Qi W, Li J, Chain YC, Pasquevich GA, Pasquevich FA, Cowan JA: Glutathione Complexed Fe/S Centers. Journal of the American Chemical Society (2012) 134(26): 10745–10748.

[61] Bekri S, Kispal G, Lange H, Fitzsimons E, Tolmie J, Lill R, Bishop DF: Human ABC7 transporter: gene structure and mutation causing X-linked sideroblastic anemia with ataxia with disruption of cytosolic iron-sulphur protein maturation. Blood (2000) 96(9):3256-64.

[62] Kushnir S, Babiychuk E, Storozhenko S, Davey MW, Papenbrock J, De Rycke R, Engler G, Stephan UW, Lange H, Kispal G, Lill R, Van Montagu M: A mutation of the mitochondrial ABC transporter Sta1 leads to dwarfism and chlorosis in the Arabidopsis mutant starik. Plant Cell (2001) 13(1):89-100.

[63] Paul DV, Lill R: Biogenesis of cytosolic and nuclear iron–sulphur proteins and their role in genome stability. Biochimica et Biophysica Acta (2015) 1853(6):1528-1539.

[64] Stojanovski D, Bragoszewski P, Chacinska A (2012): The MIA pathway: A tight bond between protein transport and oxidative folding in mitochondria. Biochimica et Biophysica Acta (2012) 1823(7):1142-1150.

[65] Sickmann A, Reinders J, Wagner Y, Joppich C, Zahedi R, Meyer HE, Schonfisch B, Perschil I, Chacinska A, Guiard B, Rehling P, Pfanner N, Meisinger C: The proteome of

*Saccharomyces cerevisiae* mitochondria. Proceedings of the National Academy of Sciences of the USA (2003) 100(23): 13207-13212.

[66] Mesecke N, Teryizska N, Koyanz Ch, Baumann F, Neupert W, Hell K, Herrmann MJ: A disulfide relay system in the intermembrane space of mitochondria that mediates protein import. Cell (2005) 121(7):1059–1069.

[67] Stojanovski D, Müller JM, Milenkovic D, Guiard B, Pfanner N, Chacinska A: The MIA system for protein import into the mitochondrial intermembrane space. Biochimica et Biophysica Acta (2008) 1783(4):610–617.

[68] Chacinska A, Pfannschmidt S, Wiedmann N, Koyjak V, Syklary KL, Schulze-Specking A, Truscott NK, Guiard B, Meisinger Ch, Pfanner N: Essential role of Mia40 in import and assembly of mitochondrial intermembrane space proteins. EMBO Journal (2004) 23(19):3735–3746.

[69] Rissler M, Wiedmann N, Pfannschmidt S, Gabriel K, Guiard B, Pfanner N, Chacinska A: The essential mitochondrial protein Erv1 cooperates with Mia40 in biogenesis of intermembrane space proteins. Journal of Molecular Biology (2005) 353(3):485-92.

[70] K. Tokatlidis (2005): A disulfide relay system in mitochondria. Cell (2005) 121:965–967.

[71] Baker MJ, Webb CT, Stroud DA, Palmer CS, Frazier AE, Guiard B, Chacinska A, Gulbis JM, Ryan MT: Structural and functional requirements for activity of the Tim9–Tim10 complex in mitochondrial protein import. Molecular Biology of the Cell (2009) 20(3):769–779.

[72] Koehler CM (2004): New developments in mitochondrial assembly. Annual Review of Cell and Developmental Biology (2004) 20:309–335.

[73] Terziyska N, Grumbt B, Bien M, Neupert W, Herrmann JM, Hell K: The sulfhydryl oxidase Erv1 is a substrate of the Mia40-dependent protein translocation pathway. FEBS Letters (2007) 581(6):1098–1102.

[74] Gross DP, Burgard CA, Reddehase S, Leitch MJ, Culotta CV, Hell K: Mitochondrial Ccs1 contains a structural disulfide bond crucial for the import of this unconventional substrate by the disulfide relay system. Molecular Biology of the Cell (2011) 22(20):3758–3767.

[75] Sideris PD, Petrakis N, Katrakili N, Mikropoulou D, Gallo A, Ciofi-Baffoni S, Banci L, Bertini I, Tokatlidis K: A novel intermembrane space-targeting signal docks cysteines onto Mia40 during mitochondrial oxidative folding. Journal of Cell Biology (2009) 187(7):1007–1022.

[76] Eliyahu E, Pnueli L, Melamed D, Scherrer T, Gerber PA, Pines O, Rapaport D, Arava Y: Tom20 mediates localization of mRNAs to mitochondria in a translation-dependent manner. Molecular and Cellular Biology (2010) 30(1):284–294.

[77] von der Malsburg K, Müller MJ, Bohnert M, Oeljeklaus S, Kwiatkowska P, Becker T, Loniewska-Lwowska A, Wiese S, Rao S, Milenkovic D, Hutu PD, Zerbes MR, Schulze-Specking A, Meyer EH, Martinou CJ, Rospert S, Rehling P, Meisinger C, Veenhuis M, Warscheid B, van der Klei JI, Pfanner N, Chacinska A, van der Laan M: Dual role of mitofilin in mitochondrial membrane organization and protein biogenesis. Developmental Cell (2011) 21(4):694-707.

[78] Lu H, Woodburn J: Zinc binding stabilizes mitochondrial Tim10 in a reduced and import-competent state kinetically. Journal of Molecular Biology (2005) 353(4):897–910.

[79] Kawano S, Yamano K, Naoé M, Momose T, Nashikawa S, Watanabe N, Endo T: Structural basis of yeast Tim40/Mia40 as an oxidative translocator in the mitochondrial intermembrane space. Proceedings of the National Academy of Sciences of the USA (2009) 106(34):14403-14407.

[80] Sideris PD, Tokatlidis K (2007): Oxidative folding of small Tims is mediated by site-specific docking onto Mia40 in the mitochondrial intermembrane space. Molecular Microbiology (2007) 65(5):1360–1373.

[81] Banci L, Bertini I, Cefaro C, Ciofi-Baffoni S, Gallo A, Martinelli M, Sideris PD, Katrakili N, Tokatlidis K: MIA40 is an oxidoreductase that catalyzes oxidative protein folding in mitochondria. Nature Structural & Molecular Biology (2009) 16(2):198–206.

[82] Stojanovski D, Milenkovic D, Müller MJ, Gabriel K, Schulze-Specking A, Baker JM, Ryan TM, Guiard B, Pfanner N, Chacinska A: Mitochondrial protein import: precursor oxidation in a ternary complex with disulfide carrier and sulfhydryl oxidase. Journal of Cell Biology (2008) 183(2):195–202.

[83] Bien M, Longen S, Wagener N, Chwalla I, Herrmann MJ, Riemer J: Mitochondrial disulfide bond formation is driven by intersubunit electron transfer in Erv1 and proofread by glutathione. Molecular Cell (2010) 37(4):516–528.

[84] Grumbt B, Stroobant V, Terziyska N, Israel L, Hell K: Functional characterization of Mia40p, the central component of the disulfide relay system of the mitochondrial intermembrane space. Journal of Biological Chemistry (2007) 282(52):37461–37470.

[85] Guo PC, Ma JD, Jiang YL, Wang SJ, Bao ZZ, Yu XJ, Chen Y, Zhou CZ: Structure of yeast sulfhydryl oxidase erv1 reveals electron transfer of the disulfide relay system in the mitochondrial intermembrane space. Journal of Biological Chemistry (2012) 287(42): 34961-34969.

[86] Becher D, Kricke J, Stein G, Lisowsky T: A mutant for the yeast scERV1 gene displays a new defect in mitochondrial morphology and distribution. Yeast (1999) 15(12):1171-1181.

[87] Lange H, Lisowsky T, Gerber J, Mühlenhoff U, Kispal G, Lill R: An essential function of the mitochondrial sulfhydryl oxidase Erv1p/ALR in the maturation of cytosolic Fe/S proteins. EMBO Reports (2001) 2(8):715-720.

[88] Coppock DL, Thorpe C: Multidomain flavin-dependent sulfhydryl oxidases. Antioxidants & Redox Signaling (2006) 8(3-4): 300–311.

[89] Dabir VD, Leverich PE, Kim S-K, Tsai DF, Hirasawa M, Knaff BD, Koehler MC: A role for cytochrome c and cytochrome c peroxidase in electron shuttling from Erv1. EMBO Journal (2007) 26(23):4801–4811.

[90] Tu BP, Weissman SJ: The FAD- and O(2)-dependent reaction cycle of Ero1-mediated oxidative protein folding in the endoplasmic reticulum. Molecular Cell (2002) 10(5):983–984.

[91] Farrell SR, Thorpe C: Augmenter of liver regeneration: a flavin-dependent sulfhydryl oxidase with cytochrome c reductase activity. Biochemistry (2005) 44(5):1532–1541.

[92] Burke PV, Raitt DC, Allen LA, Kellogg EA, Poyton RO: Effects of oxygen concentration on the expression of cytochrome c and cytochrome c oxidase genes in yeast. Journal of Biological Chemistry (1997) 272(23):14705–14712.

[93] Eckers E, Czrklaff M, Simpson L, Deponte M: Mitochondrial protein import pathways are functionally conserved among eukaryotes despite compositional diversity of the import machineries. Biological Chemistry (2012) 393(6):513-524.

[94] Lang BF, Graz MW, Burger G: Mitochondrial genome evolution and the origin of eukaryotes. Annual Review of Genetics (1999) 33: 351-397.

[95] Lister R, Hulett JM, Lithgow T, Whelan J: Protein import into mitochondria: origins and functions today (review). Molecular Membrane Biology (2005) 22(1-2):87-100.

[96] Lister R, Carrie Ch, Duncan O, Ho L, Howell AK, Murcha WM, Whelan J: Functional Definition of outer membrane proteins involved in preprotein import into mitochondria. The Plant Cell (2007) 19(11):3739-3759.

[97] Schneider A, Brusać D, Lithgow T: The direct route: a simplified pathway for protein import into the mitochondrion of trypanosomes. Trends in Cell Biology (2008) 18(1):12-18.

[98] Allen WAJ, Ferguson JS, Ginger LM: Distinctive biochemistry in the trypanosome mitochondrial intermembrane space suggests a model for stepwise evolution of the MIA pathway for import of cysteine-rich proteins. FEBS Letters (2008) 582(19):2817–2825.

[99] Ang SK, Lu H: Deciphering structural and functional roles of individual disulfide bonds of the mitochondrial sulfhydryl oxidase Erv1p. Journal of Biological Chemistry (2009) 284(42):28754–28761.

[100] Basu S, Joanne CL, Desai N, Mavridou IAD, Tang HK, Goddard DA, Ginger LM, Lukeš J, Allen WAJ: Divergence of Erv1-associated mitochondrial import and export pathways in Trypanosomes and anaerobic protists. Eukaryotic Cell (2013) 12(2):343-355.

[101] Eckers E, Petrungaro C, Gross D, Riemer J, Hell K, Deponte M: Divergent molecular evolution of the mitochondrial sulfhydryl: cytochrome c oxidoreductase Erv in Opisthokonts and Parasitic Protists. Journal of Biological Chemistry (2013) 288(4):2676–2688.

[102] Carrie Ch, Giraud E, Duncan O, Xu L, Wang Y, Huang S, Clifton R, Murcha M, Filipovska A, Rackham O, Vrielink A, Whelan J: Conserved and novel functions for *Arabidopsis thaliana* MIA40 in assembly of proteins in mitochondria and peroxisomes. Journal of Biological Chemistry (2010) 285(46):36138–36148.

[103] Deponte M, Hell K: Disulphide bond formation in the intermembrane space of mitochondria. Journal of Biochemistry (2009) 146(5):599-608.

[104] Wirtz E, Leal S, Ochatt C, Cross G: A tightly regulated inducible expression system for conditional gene knock-outs and dominant-negative genetics in *Trypanosoma brucei*. Molecular and Biochemical Parasitology (1999) 99(1):89–101.

[105] Poon KS, Peacock L, Gibson W, Gull K, Kelly S: A modular and opitimized single marker system for generating *Trypanosoma brucei* cell lines expressing T7 RNA polymerase and the tetracycline repressor. Open Biology (2012) 2(2):110037.

[106] Brun R, Schönenberger M: Cultivation and *in vitro* cloning of procyclic culture forms of *Trypanosoma brucei* in a semi-defined medium. Acta Tropica (1979) 36(3):289-92.

[107] Dean S, Sunter J, Wheeler JR, Hadkinson I, Gluenz E, Gull K: A toolkit enabling efficient, scalable and reproducible gene tagging in trypanosomatids. Open Biology (2016) 5:140197.

[108] Clark P. David, Molecular Biology: *Understanding* the Genetic Revolution. United Kingdom: Elsevier, Inc., © 2005. 784 p. ISBN: 0-12-175551-7.

[109] Moore BC, Guthrie HE, Huang M, Taxman JD: Short Hairpin RNA (shRNA): Design, Delivery, and Assessment of Gene Knockdown. Methods in Molecular Biology (2010) 629:141–158.

[110] Tong WH, Rouault TA: Metabolic regulation of citrate and iron by aconitase: role of iron-sulphur cluster biogenesis. BioMetals (2007) 20(3-4):549-564.

[111] Saas J, Ziegelbauer K, von Haeseler A, Fast B, Boshart M: A developmentally regulated aconitase related to iron-regulatory protein-1 is localized in the cytoplasm and in the mitochondrion of *Trypanosoma brucei*. Journal of Biological Chemistry (2000) 275(4):2745-55.

[112] Bisswanger H: Enzyme assays. Perspectives in Science (2014) 1(1-6):41-55.

[113] Perry WS, Norman JP, Barbieri J, Brown BE, Gelbard AH: Mitochondrial membrane potential probes and the proton gradient: a practical usage guide. Biotechniques (2011) 50(2):98–115.

[114] Rottenberg H, Wu S: Quantitative assay by flow cytometry of the mitochondrial membrane potential in intact cells. Bichimica et Biophysica Acta (1998) 1404(3):393-404.

[115] Hardin Ch, Edwards J, Riell A, Presutti D, Miller W, Robertson D, Cloning, Gene Expression, and Protein Purification: Experimental Procedures and Process Rationale. New York: Oxford University Press, Inc., © 2001. 435 p. 00-045312.

[116] Panigrahi AK, Zíková A, Dalley R, Acestor N, Ogata Y, Anupama A, Myler PJ, Stuart KD: Mitochondrial complexes in *Trypanosoma brucei*: a novel complex and a unique oxidoreductase complex. Molecular & Cellular Proteomics (2008) 7(3):534–545.

[117] Chevallet M, Luche S, Rabilloud T: Silver staining of proteins in polyacrylamide gels. Nature Protocols (2006) 1(4):1852–1858.

[118] Senbongi H, Ling F, Shibata T: A mutation in a mitochondrial ABC transporter results in mitochondrial dysfunction through oxidative damage of mitochondrial DNA. Molecular & General Genetics (1999) 262(3):426-236.

[119] Stojanovski D, Rissler M, Pfanner N, Meisinger C: Mitochondrial morphology and protein import—A tight connection?. Biochimica et Biophysica Acta (2006) 1763(5–6):414–421.

[120] Ozer HK, Dlouhy AC, Thornton JD, Hu J, Liu Y, Barycki JJ, Balk J, Outten CE: Cytosolic Fe-S Cluster Protein Maturation and Iron Regulation Are Independent of the Mitochondrial Erv1/Mia40 Import System. Journal of Biological Chemistry (2015) 290(46):27829-40.